Experimental Investigation for Process Optimization during Gas Metal Arc Welding of Al-6063 alloy

A Dissertation submitted
in partial fulfillment of the requirements
for the degree of

Master of Engineering

in

Production Engineering

by

Rahul Varshney
(801382020)

Under the Supervision of
Dr. Anirban Bhattacharya
Assistant Professor

MECHANICAL ENGINEERING DEPARTMENT

THAPAR UNIVERSITY, PATIALA

July, 2015

CERTIFICATE

I hereby declare that the thesis entitled "**Experimental Investigation for Process Optimization during Gas Metal Arc Welding of Al-6063 alloy**" is an authentic record of my work carried out as requirements for the award of the degree of **Master of Engineering** in **Production Engineering** at **Thapar University, Patiala** under the supervision of **Dr. Anirban Bhattacharya**, Assistant Professor, Mechanical Engineering Department, Thapar University, Patiala during July, 2013 to July, 2015. No part of the matter embodied in this report has been submitted to any other university or institute for the award of any degree.

Date: 13-07-2015

Rahul Varshney

It is certified that the above statement made by the student is correct to the best of my/our knowledge and belief.

Dr. Anirban Bhattacharya
Mechanical Engineering Department
Thapar University, Patiala - 147004

Countersigned by

Head, Mechanical Engineering Department
Thapar University, Patiala – 147004

Dean of Academic Affairs
Thapar University, Patiala - 147004

Acknowledgement

It gives me a great sense of pleasure to present the report of the thesis work undertaken during ME second year. I owe special debt of gratitude to **Dr. Anirban Bhattacharya, Assistant Professor, Department of Mechanical Engineering**, for his constant support and guidance throughout the course of our work. His sincerity, thoroughness and perseverance have been a constant source of inspiration for us. It is only his cognizant efforts that our endeavors have seen light of the day.

I also take the opportunity to acknowledge the contribution of **Dr. S.K. Mohapatra, Senior Professor and Head, Department of Mechanical Engineering** for his full support and assistance.

I also do not like to miss the opportunity to acknowledge the contribution of all faculty members of the department for their kind assistance and cooperation. Last but not the least, I acknowledge my friends for their contribution in this work.

Thanking you.

Rahul Varshney

(801382020)

Abstract

Aluminum alloys are commonly used in automobile industries, ship and marine sectors because they are light in weight, high corrosion resistance. Since very large parts are made so they need to be joined by welding. MIG welding is commonly used for Al alloy because it produces spatter free welding, high deposition rate and easy to operate. The quality of the weld depends on the factors of the welding. Proper combination of welding parameter is necessary to get the better result. So optimization of the welding parameter is necessary.

In this study various MIG welding parameter like current, voltage, gas flow rate, groove angle and post weld aging was taken to study and analyze. L18 orthogonal array was used for experimental trials. Taguchi method was used to optimize the results. Signal to noise ratio was also found for analyze the parameter effect. Tensile strength, toughness and microhardness in fusion and heat affected zone were done to find out the various outcomes at different experiment level. SEM and optical microscope was used to analyze the metallurgical effect of welding parameters. Grey relation analysis was used to find out the best result for different outcomes of the weld joint.

Table of contents

LIST OF FIGURES

LIST OF TABLES

Nomenclature

Y = Grey relation coefficient

N_{ij} = Normalization of various responses of experimental trial

N = total number of experiments

$\bar{m}$ = Average response of different experiments trials

μ_{opt} = Desired mean value

V_e = Variance of error

X_{ij} = Response value at different experiment trials

Greek Symbols

Δ = Absolute difference between N_{oj} and N_{ij}

Acronyms

ANOVA = Analysis of Variance

FZ = Fusion zone of weld metal

HAZ = Heat affected zone of weld metal

DF = Degree of freedom of a factor

CHAPTER-1

Introduction

1.1 Introduction

Welding of Al-Mg alloy is important because it is used in automobile and marine field where very large components are formed. Basically Al-Mg alloys are used in this field because they are economical and light weight. Besides these properties, Al-Mg alloys have good temperature resistance property, good toughness and strength. Basically the welding of Al-Mg is not easy due to the formation of oxide layer and some other problems. One of the arc welding process which is metal inert gas (MIG) welding process that is highly used in industries for welding Al-Mg alloys because of optimum welding quality, minimum distortion, it can be done in all positions and it is economical.

1.2 Different Al-Mg alloys

Based on their composition Al-Mg alloys are classified in different four digit grade alloy. Every grade alloy has its own specification and its own practical applications.

1.2.1 Al-Mg 5xxx grade alloys

As comparison to other alloy, 5xxx series alloy contains maximum magnesium content. Besides magnesium, it also has Mn, Fe and some other element. The amount of magnese increases the hardenability of alloy. It has a very good weld quality and high corrosion resistance. It is used for making high ship parts. It also contains good mechanical properties. The most common alloys of 5xxx series which are used in industries are Al- 5052, 5083, 5086 etc.

1.2.2 Al-Mg 6xxx grade alloys

The most common alloys which are used in making general purpose products are 6xxx series grade alloys. These alloys contain magnesium and silicon as a major element. These alloys have an advantage that these alloys are heat treatable. This is why it is mostly used in welding because it recovers its mechanical properties after post weld heat treatment. The heat

treatment is done according to T6 method in which Mg_2Si precipitates are formed. The most common alloys of 6xxx series are Al 6063, 6061. These alloys have good weldability and good mechanical properties.

1.2.3 Al-Mg 7xxx grade alloys

In this grade alloys, zinc is the major constituent besides aluminum. It also contains copper, chromium, magnesium and magnese. It is generally used in air frame parts, mobile parts and some high strength aerospace parts. It can be aged after welding to increase the strength of the joint.

1.3 Al-Mg binary phase diagram

Fig. 1.1 shows the state of Al-Mg alloy at different temperature. It also shows the different alloys formation at different temperature and state. It also helps in selecting different welding parameter.

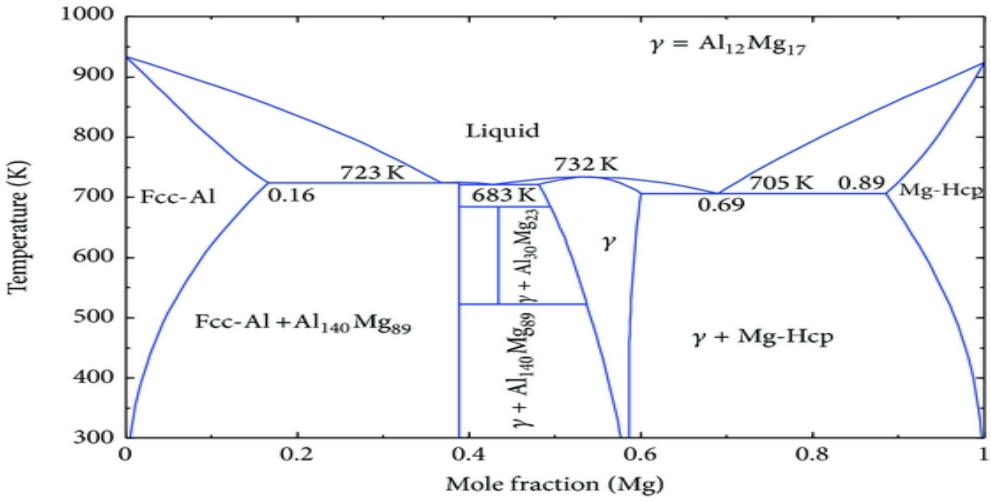

Figure1.1: Binary phase diagram of Al-Mg alloy (Web reference1)

Many assessments have been done for the binary aluminum-magnesium phase diagram, both in terms of theoretical calculations and experimental observation. There is a small amount of variation between these assessments but they largely agree. This is found that γ-phase exists in range of 48-55 at % aluminum and the β-phase exists at 60-63 at% aluminum, although the exact composition ranges of the two phases has been reported with minor discrepancies, as has the formation of other phases. The β-phase is reported to have a narrow composition

range at, or close to, 61.5 at% aluminum (38.5 at% magnesium) and to undergo the eutectic reaction, (Al) + Al_3Mg_2 → L, at the eutectic temperature of 450 °C. The γ-phase composition range varies slightly in the nature, particularly at low temperatures and is usually given the composition $Al_{12}Mg_{17}$ - or, less often, Al_2Mg_3 - despite its large solubility range. It undergoes the eutectic reaction, (Mg) + $Al_{12}Mg_{17}$ → L, at the eutectic temperature of 437 °C.

The solubility of aluminum in the γ-phase increases with increasing temperature from 48.1 at% Al at 350 °C to 54.2 at% Al at 445 °C. The existence of a third phase is also widely accepted. Its composition is thought to be around 44 at% Mg or 42 at% Mg, and is quoted as being between 43.5- 44.8 at% Mg. This phase is commonly called the R phase but is sometimes referred to as the ε phase and is thought to form either via the peritectic reaction, L + ζ → R, or via the peritectoid reaction, β + γ → R, at a temperature of 410 °C. A ζ-phase was included in the phase diagram from but is not widely included in other works.

This phase has $Al_{52}Mg_{48}$ and existing in the temperature range 410 – 452 °C. Similarly a λ-phase having a composition of 42.5 at% Mg and exist between 450 °C and 435 °C, forming via a peritectic reaction (L + γ ↔ λ) and dissociating into β and γ between 435 and 425 °C.

1.4 Welding of Al- Mg alloy

Since Al-Mg alloys used for making higher automobile parts so it requires permanent joining by welding. Some mechanical properties of alloy get reduced but it can be compensated by post weld heat treatment. The problems in the welding of Al-Mg alloys are as following

- Al-Mg alloy welding depends upon its composition because an alloyed element highly affects the property of welding joint.
- Al-Mg alloy has high thermal conductivity which means heat is easily transferred from the welding zone. So a very powerful source is required which reaches to its melting point easily so that the proper heat should be given to weld zone. Higher thermal conductivity also affects the zone which is near to the weld zone.
- Al-Mg alloy has higher coefficient of thermal expansion. This is why distortion and stress are generated in the weld if it is not done properly.
- Aluminum usually does not change in color when it is heated. This creates problem in welding.
- Al-Mg alloys are highly reactive because they form oxide very easily.

- Al-Mg welded joint does not have a very good strength. When it is stressed, it generally breaks or distorts from the weld joint.
- Welding of Al-Mg alloys requires very high cleaning practice so a very high skilled man is required for welding.

Due to these difficulties every welding is not possible for Al-Mg alloys. For the welding of Al-Mg alloy, mostly MIG welding, TIG welding and friction stir welding is used. These welding have following advantages

- Prevent oxidation
- Gives high precision
- High capacity of electrode
- Provide better quality
- Produces spatter free welding

These all welding are suitable to Al-Mg alloy but MIG welding is chosen for study purpose because it produces spatter free welding and it is economical. The description of MIG welding is given in section 1.5

1.5 Metal Inert Gas (MIG) Welding

Welding has many types like arc welding, resistance welding, solid state welding, thermit welding etc. They all are used according to their specific applications. MIG welding is the type of arc welding process. In this section working principle, equipments, advantages, disadvantages and application of MIG welding are described in detail.

1.5.1 Equipments and working principle

MIG welding is a semi-automatic or automatic arc welding process in which arc is generated between electrode and work piece due to continuous feed of wire from the spool. In general, constant voltage source with direct current (DC) is generally used but constant current with alternating current power source can also be used. It works on the principle of arc generation in which ions are transferred from electrode to work piece. In this work piece is connected to one terminal and electrode is connected to another terminal.

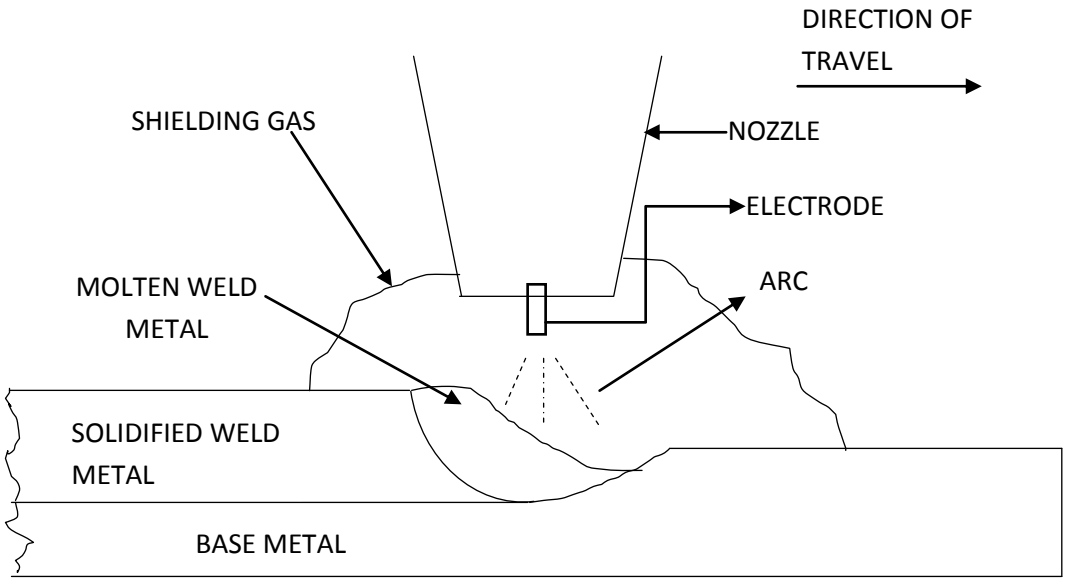

Fig 1.2: Schematic diagram of MIG Welding Process

The equipments used in this process are:

- **Power Source**

Generally MIG welding uses a constant voltage power supply. In this welding, arc length variation changes the heat input and current so shorter arc length causes great heat input and better results. In this welding both AC and DC source can be used but generally DC source is generally used with electrode positive polarity.

- **Wire feed unit**

The wire feed unit supplies the electrode wire at a constant speed from the spool to the contact tip of welding torch. The speed of wire transfer depends upon the size of the weld and the arc voltage. The wire transfer also depends on the DC motor.

- **Welding Torch**

The welding torch delivers electrode wire to the place where welding is required. The torch consists of a control switch, contact tip, power cable, nozzle and liner. The wire comes from contact tip and move through the liner, it reaches to work piece. The torch may be air cooled or water cooled. In air cooled torch, gas flows from the side of the liner. But in water cooled system, there is separate system for each purpose.

- **Shielding gas**

In MIG welding, the most common inert gas used are Ar, He or mixture of both gas. The main purpose of using the inert gas is to protect the metal from atmospheric gases. The selection of the shielding gas depends upon the composition and size of the weld metal.

1.5.2 Advantages of MIG Welding

MIG welding is mostly used in industries because it can weld a variety of materials. Some advantages of MIG welding which are discussed below

- MIG welding is faster as compare to other welding because wire is fed continuously.
- It can weld both thin and thick materials.
- It has high deposition rate so it can be used for deep penetration.
- It can be automatic or semi automatic according to the need. So it is very flexible.
- It does not require any flux to remove.
- It gives clean, smooth, stable and high quality weld.
- Due to high travel speed, it generates less distortion.
- It generates fewer amounts of fumes.
- It can weld in all positions.
- It can weld both ferrous and non ferrous metals.

1.5.3 Disadvantages of MIG welding

There are some disadvantages of MIG welding which are discussed below.

- The equipments of MIG welding are complex and they are difficult to understand.
- It generates unstable arc. Due to this it produces burn back.
- It is not suitable for outdoor applications because air can disturb its shielding gas envelope.
- In this welding there is a problem of irregular wire feed.
- There is a possibility of porosity, incomplete fusion and crack in MIG welding.

1.5.4 Applications of MIG welding

- It can weld a variety of materials like both low and high alloy, ferrous and non ferrous material, aluminium, titanium and other materials alloys.
- It can be used for automotive repair and pipe joints.
- It is used in industries for making large products like pressure vessel, ship parts and other automobile parts.
- It is used in refrigeration industry.

1.6 Organization of thesis work

The thesis work has been divided into five chapters. Chapter 1 covers the basic information of MIG welding and Al-Mg alloy and its application. It also covers the requirement of welding, difficulties in welding of Al alloy. It also contains different phase of Al-Mg alloy. Chapter 2 contains different literature review which shows recent development and future possible study in that work. Chapter 3 includes selection of orthogonal array, pilot experimentation, selection of factor. In this chapter different tests and methodologies are described in detail. Chapter four contains experimental results and interpretation of the results. This chapter also deals with graphical results, Taguchi method and signal to noise ratio and grey relational analysis. Chapter five contains all conclusions and future scope of the study.

CHAPTER-2

Literature Review

2.1 Introduction

In this chapter, there are some literature reviews based on previous works related to the welding of Al-Mg alloy. Different welding methods like MIG welding, TIG welding and friction stir welding are studied and their results are discussed in this chapter. These literature reviews show different results at different parameter level by using different techniques. These research papers can be categorized into 3 types.

First one in which study was focused on modelling of welding joint and its behaviour with time and joint location variation. Second one in which microstructure and mechanical properties were concerned. Third one shows the post weld heat treatment effect on weld joint.

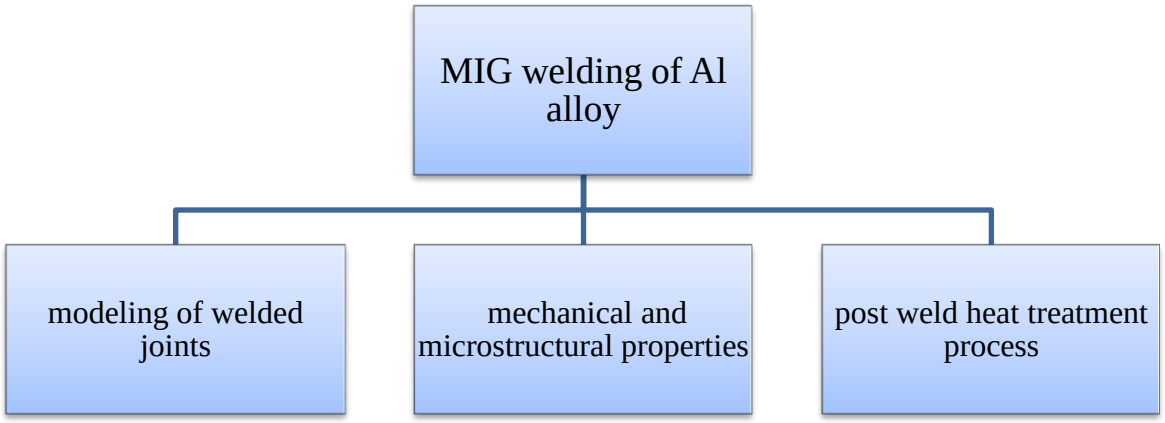

Fig 2.1: Literature review chart

2.2 Review of Literature

In this section, reviews of different journal papers which are related to welding of Al-Mg alloy have been discussed.

2.2.1 Modeling of Weld Joints

Dutta and Pratihar [2006] investigated the analysis of TIG welding modeling using regression and artificial neural network approach. In regression analysis, they calculated the input and output parameters. With the help of this analysis, many data were created at random within certain range and for that data, different response and outcomes were calculated for every combination of input. There are different methods of neural network like genetic algorithm neural network and back propagation neural network. Both regression analysis and neural network approaches were compared for different responses. It was seen that neural network approaches are more adaptive in nature. Genetic algorithm provides better results as compare to back propagation method.

Ghosh et al. [2007] studied arc behaviour and metal flow properties in Al alloy welded by pulsed current MIG welding. During all experiments, a high speed video photography was done to completely understand the arc behaviour in joint. It was found that mean current, arc voltage and a dimensionless number φ = [(pulse current / base current) x pulse x off time x pulse frequency] affects the arc behaviour at different parameters level. These help in determining the mathematical expression of root diameter, projected diameter and length, velocity of droplet and deposition in weld pool. The mathematical expression provides almost accurate result as comparison with experimental results.

Guo et al. [2009] studied the crater formation in MIG welded aluminium alloy. Both mathematical modelling and experiments were performed to predict the behaviour of weld pool in welding. Mass, momentum and energy equations with different boundary conditions were used to predict the crater force, area, formation time and temperature at different location. A simulation was also used to check the temperature behaviour of crater in welding joint. Some experiments were also conducted to check crater behaviour and validate with mathematical modelling. It was found that experimental results and numerical modelling gives almost approximately same results. It was found that crater is formed at the end of the weld plate because fast solidification takes place before molten metal back up. So solidification crack occurs at centre. A back up technique was suggested to overcome this problem.

Traidia and Roger [2010] investigated a finite element model to find out the relation between arc type and arc flow characteristics. Different zone were studied for this purpose like cathode zone, anode zone and arc formation zone. For these regions, different time model were made which defines heat transfer characteristics, arc flow characteristics and electromagnetic field behaviour. The model shows the behaviour of arc and formation of weld pool and shows the eddy current value in different region. Behavior of weld pool in the case of full penetration was also observed. For checking the results, an infra red camera was used. This makes an algorithm which shows the behaviour of weld pool at different time and locations of weld region. This algorithm was used on TIG welding steel samples. It was find that numeric and experimental results match with each other. There is an important role of marangoni effect in weld pool behaviour study.

Li et al. [2011] studied weld pool shape variations under different welding parameters (speed, arc length and current). These different parameters were taken at different levels on TIG welding of martensitic steel plate. Different kinds of weld pool shape are formed at different level. These shapes were analyzed on the basis of their mechanism formation. It was found that marangoni convection plays a significant role for weld pool shape formation. It was studied that inward marangoni causes the molten metal to flow in the weld pool. Thus deep shaped weld pool forms. Double shielded arc method was suggested because it converts the outward flow into inward flow. This makes weld pool deep and narrow.

Qin et al. [2015] described the numerical simulation on MIG welding of aluminium to galvanized steel. The welding was done with the help of difference in melting point between aluminium and steel. The MIG arc was treated as Gaussian model. Numerical analysis was done with the help of heat energy equation. The heat input was calculated a different voltage and current level. Different boundary conditions were used to get the appropriate results. The simulation was done with the help of ANSYS software. With the help of ANSYS, temperatures at different locations were obtained. It was found that results of both numerical and simulation are approximately same. It was also suggested that backing plates should be provided to Al plates and it was also found that temperature distribution is not symmetrical to weld plates.

2.2.2 Mechanical and Microstructural Properties

Senthil et al. [2006] studied the effect of different welding parameters on corrosion property of the TIG welded aluminium alloy joint. Pulse related parameter like pulse

frequency, pulse current, pulse on time and base current was chosen as a parameter levels. These parameters help in improving mechanical properties. A mathematical model was developed to show behaviour of joint at different level. Factorial experimental design, ANOVA and regression method was used to optimize the experimental conditions. Finally from the calculations it was found that on increasing pulse current and pulse frequency, pitting corrosion also increases. It was also found that on increasing base current and pulse on time, pitting corrosion decreases.

Aesh [2007] studied welding parameter variation on weld bead dimensions of TIG welding aluminium alloy joint. For this, welding current, welding speed, vertex angle and electrode diameter were chosen as a factor on the study of weld pool dimensions. It was found that on increasing the current weld bead dimensions also increase. It was also found that current is not an independent factor. It highly depends on welding speed. It was found that welding current and welding speed have inverse proportional relationship. It means on increasing the welding current, welding speed decreases. It was also found that weld bead quality highly depends on welding speed. Welding speed should be proper so that arc can get proper time to fill the bead in weld pool. If the welding speed is proper, then deep weld bead gets generated. Very fast and slow speed reduces the quality of the bead. It was found that on increasing the apex angle, weld bead width increases. It was also found that on increasing the electrode diameter weld bead decreases.

Balasubramanian et al. [2007] studied the pulsed current effect on Al-Mg-Zn alloy joint. Both continuous current and pulsed current MIG and TIG welding were used to join the plates. Both mechanical and micro structural properties were examined. It was found that all the mechanical properties like ultimate strength, hardness and toughness are more in case of pulsed current welding as compare to continuous current welding. The morphological study was also done. It was seen that in continuous current welding, there is no fine grain structure while in pulsed current welding, there is fine grain structure in both fusion and heat affected zone.

Lakshminarayan et al. [2007] studied effect of tensile properties on aluminium 6061 welded joint. The welding techniques used were MIG welding, TIG welding and friction stir welding. It was found that friction stir welded joint has better tensile properties and joint efficiency is also better in FSW welding. MIG welded joint has lower tensile properties as comparison of other two processes. From morphology study, it was found that FSW joint has finer, uniformly distributed equiaxed granular structure while in case of MIG and TIG welding, the grains are big in size. It was found that high heat in MIG welding causes large

size dimples in his fractured morphology. TIG welding and friction stir welding generates low heat input so their tensile strength is better than MIG welding.

Maggiolino and Schmid [2007] studied the corrosion resistance effect on AA6060T5 and AA6082T6 weld plates. A comparison between friction stir welding and metal inert gas welding was studied morphologically. First all the samples were cleaned, polished and etched with NaOH solution. Then they were dipped in a water solution of acetic acid and sodium chloride maintaining temperature 65° - 67° C. After soaking 3 hours, the numeric and areal densities of picture area were calculated. With the help of this, index value was calculated for all pieces. It was found that there is no difference in base metal structure. But in weld plates it was found that MIG plates have higher index values so it contains more critical zone.

Manti and Dwivedi [2007] studied the effect of different welding parameters on the Al 6xxx series alloy. Peak current, pulse duration and pulse frequency were selected as a factor. The study was done on both fusion zone and heat affected zone. It was found all these parameter affects the microstructure property and there is proper relation between these parameters and microstructure grains. Due to welding, secondary precipitates are generated in the grain boundary due to which coarsening of aluminium grains take place. These precipitates affect the quality of microstructure. It was found that on increasing the pulse frequency, the size of the grains gets reduced which affects the mechanical properties of the welding joint. It was found that on increasing these parameters, different effect are found in fusion zone and heat affected zone. It was found that fusion zone is more sensitive compare to heat affected zone. The effect of pulse duration and pulse current was also found in microstructure properties of the joint. It was found that higher pulse current and longer pulse duration makes grains coarse in both fusion and heat affected zone.

Sugamata and Kaneko [2007] studied the different mechanical properties variation in normal and high temperature. For this study a heavy plate of aluminium and magnesium alloy was taken and TIG welding was done on that plate. Both base metal and weld joint were taken for the study and properties were measured at different temperature. In tensile and impact test, there is no difference in properties at normal and high temperature on base and weld metal. But there is difference in the creep and fatigue test of base and weld joint at normal and higher temperature. It was found that tensile strength of base metal and weld metal at different temperatures are same. But in elongation case the base metal elongation increases at higher temperature. At high temperature failure takes place early in the weld region from necking. So creep time and creep fracture elongation is low at high temperature.

In high temperature creep deformation, different cavities are formed in the microstructure and these cavities combine with each other and deformation takes place from the weld region.

Kumar and Sundarrajan [2008] studied the mechanical properties of TIG welded Al alloy welding joints. Taguchi method was employed to optimize the different parameters of welding so that mechanical properties of the welded joint can be improved. Base current, welding speed, pulse frequency and pulse speed were chosen as the welding factor for the study. Regression model was developed to predict the welding parameter behaviour. ANOVA was formed to find out the significance of each factor. Microstructural study was also done on the weld joints and different mechanical properties at different parameter level were correlated to each other. From the ANOVA table, it was found that pulse frequency is the highest significant factor for all mechanical properties. Beside this the interaction of welding speed and current are also significant factor for the study. The study of planishing was also done for the welded joints and it was found that it improves the mechanical properties because it relieves the internal stress generated in the joint.

Rui et al. [2008] studied the dynamic progress and residual distortion of out-of-plane of aluminium alloy 5A12 was investigated under different welding conditions of TIG welding. The dynamic out-of-plane distortion was measured by self-developed distortion measuring system. Out-of-plane distortion mechanism and the effecting parameters on distortion process were analyzed, and the effect of plate thickness and welding heat input on distortion was discussed. The results show that besides welding parameters, base metal thickness and welding heat input has high effect on distortion on the joint. The residual distortion of out-of-plane can be divided into three types including arch, buckling and bowling distortion.

Zhao et al. [2009] compared the results of TIG welding and FSW welding for the Al-Mg-Sc alloy plates. Different tests were done on the welding joint like tensile strength, optical microscope, scanning electron microscope and Vickers microhardness. From the results it was found that friction stir welding gives better results compare to TIG joint. This happens because low heat generated in friction stir welding as compare to TIG welding so particles of Al_3 (Mg-Sc) particles are preserved in the microstructure of the joint. Besides this, it was found that friction stir welding has a fine grain structure which is not available in TIG welding grains. These grains play a significant role in the properties of welded joint.

Kim et al. [2010] studied corrosion and mechanical properties of MIG welded Al-5083 alloy. Based on slow strain rate, electrochemical tests were done on Al plate at different potential level in natural aerated sea water. The variation of current density with applied

potential was checked and also a curve was drawn between percentage elongation and strength with applied potential to check the best and optimum properties. Results show that optimum corrosion potential for better mechanical properties lie between -1.2 V to -0.7 V. The fracture morphology was also done after slow strain rate test. It was found that for optimum potential range, a dimple pattern and shear lips were observed. Ductile fracture behaviour with dimple pattern was observed at -1.35 V.

Salazar et al. [2010] studied micro structural and mechanical properties of aluminium 6061 and 7020 welded joint by TIG and MIG welding. For this optical microscopy, scanning electron microscopy and Vickers hardness tests were done in both transverse and longitudinal direction. Micro analytical studies were also carried out by using an electronic microprobe. In SEM, it was found that there is a dendritic characteristic in molten pool of both Al 6061 and 7020 alloys. There is an indendritic phases in Al 6061 but it is not available in Al 7020. From electronic microprobe, it was found that there is no loss of alloying elements. From Vickers hardness test, a curve was drawn between hardness and distance. It was found there is same nature in the variation of hardness in HAZ in both Al 6061 and Al 7020 alloy.

Mutombo and Dutoit [2011] studied the corrosion-fatigue properties of weld joint of Al alloy. It was done with the help of automatic gas metal arc welding and filler alloy was ER 5183. In this SEM and EDS analysis were performed. In this welding machine parameters were arc voltage, welding current wire parameters were wire feed speed, wire diameter and some other parameter like nozzle to plate distance, travel speed, torch angle and gas flow rate were considered. SEM and EDS were done on the different zone of welding like fusion zone, heat affected zone and parent metal portion. There is coarse granular structure at fusion zone and equiaxed structure is formed at heat affected zone. It was found from the results that weld joints failed at the interface because of high pitting rate. The fatigue life was found to be reduced when it is immersed in NaCl as compared to ambient air.

Shiang et al. [2011] studied the optimization of welding parameters for Al foam plates weld by MIG welding. Multi- response objective method was used for this study. Principle component analysis was chosen as a method for this study. Al foam plate was taken and compression testing machine was used. Parameters were filler material, MIG current, welding speed, MIG gas flow rate, work piece gap, MIG arcing angle. SEM and EDX were used to get composition. Performance characteristics were bending strength and micro hardness. Optimum solution was found by Taguchi method.

Dongxia et al. [2012] studied microstructure of TIG welded Al-Mg alloy with Erbium (Er) addition. Optical microscopy and x-ray diffractometer was used to analyze micro

structural examination and phase analysis respectively. It was seen in structure that round precipitate of Al_3Er was distributed in the base metal but in weld metal, these precipitates are found near fusion zone which increases grain refinement in this region. Backscattered images were also studied and there were presence of bright white block dot points of Al_3Er in the fusion zone. Near fusion zone, an equiaxed grain structure was found.

Vargas et al. [2013] investigated mechanical properties variation in Al alloys plate of MIG welding. For this yield strength and micro hardness were measured before and after welding. The study was done by taking heat input as a prime factor. A thermal transient model was developed to calculate heat input rate at various parameter level by using FEM technique. Different models were created and compared with each other and it was also compared with experimental results. Different graphs were plotted between temperature and distance in fusion line at different heat input level. It was observed that heat input influences the maximum temperature reached by Aluminium which affects the mechanical properties of plate. This happens due to the transformation of β˝ to β′ particles and Mg_2Si precipitates.

Mathivanan et al. [2014] studied the comparison of pulsed and dual pulsed MIG welding on Al 6061 plates. Dual pulsed contains pulsed current and thermal pulsation. Both mechanical and micro structural properties were compared. From XRD radiography, it was found that dual pulsed welded joint has less amount of hydrogen content so there is a less amount of porosity. It was found that dual pulsed joint has less coarse grain structure. Dual pulsed joint has also better mechanical properties.

Wei et al. [2014] studied the heat input effect on pulsed MIG welded joint. At different heat input, microstructure of joints was investigated. It was found that at low heat input, there is a serrated layer in structure. At high heat input, different precipitates were formed like $TiAl_3$, $Ti_7Al_5Si_{12}$ and α-Ti in microstructure. EDS shows that weld is composed of α-dendrites and Si- eutectic phase. Some $TiAl_3$ precipitates structure was seen in structure which affects the quality of weld. As heat input increases, the number of precipitates decreases but the size of precipitate increase. It was found that for a particular range of heat input, weld without defect is obtained.

Yanet et al. [2014] investigated the variation in mechanical properties of the Al-Mg alloys welded by laser-MIG hybrid welding. The results were compared with MIG welding. There were 3 causes of strength loss which are solute strengthening, precipitate hardening and grain boundary strengthening. The result shows that tensile strength and fatigue strength is better in Laser MIG welded joints. SEM and TEM were also done on the fractured surface. It was found that loss of strength in the weld joint due to vaporization of Mg particles. The

main reason for loss in fatigue strength is porosity in the welding. It was also found that fusion zone is the weakest part of the joint.

2.2.3 Post Weld Heat Treatment Process

Ahmad and Bakar [2011] studied the effect of post weld heat treatment on Al 6061 joint welded by MIG welding. In this cold metal transfer was used because it produces spatter free welding. The samples were divided into two categories (a) simple welded samples (b) post weld heat treatment samples . The PWHT samples were heat solutionised at 530° C for 1 hour and after this they were artificially aged at 160° C for 20 hours. All the samples were tested at UTM machine at 100 kN. Besides this all the samples were tested on the Vickers hardness testing machine at 0.2 kg load at top, centre and bottom area of weld zone. SEM analysis was used to see the tensile fracture of specimen at top, centre and root area. From the results, it was found that there is an increment in average hardness value and tensile strength. The tensile failure occurs from heat affected zone area and there is fine dimples structure in PWHT samples as comparison to simple welded samples which shows the ductility of material.

Temmar et al. [2011] studied post weld aging effect on TIG welded Al 7075 plates. Aging was done at 140° C for soaking time of 10 hours. Tensile strength, impact energy and Vickers micro hardness tests were done on the weld samples and post weld aging samples. It was found there is an increment in ultimate strength and impact energy in post weld aging samples as compared to welded samples although their values are low as comparison to base metal. It was seen that hardness values increase from fusion zone to heat affected zone region. SEM was done on the fractured surface of impact test specimen. It reveals some cleavage facets which indicate its brittle nature. Some dimples, inter granular fracture features was observed in the SEM.

Cheema et al. [2014] studied post weld heat treatment effect on TIG welded Al alloy joints by taking mechanical and metallurgical properties into consideration. There were 4 cases of welding which are simple welded joints, welded joint with solution heat treatment, welded joint with artificially aging and welded joint with solution heat treatment and aging . Artificially aging was done at 175° C for 10 hours and solution heat treatment was done at 500° C for 4 hours and then rapid quenching. It was found that better tensile strength and fatigue strength was achieved in case of artificially aged joints. In optical microscopy, every joint was seen at fusion zone and heat affected zone.

2.3 Literature Summary

The literature review presented in section 2.1 shows the different mathematical model for predicting the behaviour of different responses like crater behaviour [Guo et al., 2009], metal transfer, heat transfer and fluid flow in weld region [Traidia and Roger, 2010]. These mathematical models were compared with simulation software to validate the result [Qin et al., 2015]. Some previous studies focussed on the heat behaviour in joint so that minimum defects occur in the weld [Ghosh et al., 2007; Qin et al., 2015]. In some studies, modern technology like high quality photo videography and infra red camera was used to study the weld pool dynamic behaviour [Traidia and Roger, 2010; Li et al., 2011]. Some programmable method like finite element method, neural network, and back propagation method were used so that multiple iterations can be solved easily. [Dutta and Pratihar, 2006]. Effect of welding parameters like current, voltage, gas flow rate, welding speed were studied so that better mechanical properties can be achieved [Senthil et al., 2006; Aesh, 2007; Manti and Dwivedi, 2007]. Different welding techniques like MIG welding, TIG welding and Friction stir welding were used to find out the better properties and structure in the weld [Yanet et al., 2014; Salazar et al., 2010; Zhao et al., 2009; Maggiolino and Schmid, 2007; Lakshminarayan et al., 2007; Balasubramanian et al., 2007]. Mechanical properties like tensile strength, impact strength and micro hardness were studied. Effect on alloying element on the surface structure and mechanical properties were also studied [Zhao et al., 2009; Dongxia et al., 2012]. SEM, EDS and XRD were used to study the micro structure in base metal, weld zone and fractured zone to analyze the metal behaviour [Wei et al., 2014; Mathivanan et al., 2014; Dongxia et al., 2012]. Effect on grains and precipitates due to change in heat input and temperature were also analyzed. Some literature review shows the effect of post weld heat treatment on weld joint in terms of mechanical and micro structural properties [Ahmad and Bakar, 2011; Temmar et al., 2011; Cheema et al., 2014].

2.4 Scope and objectives of the present Study

The scope and the requirement for this study could be well explained by understanding the application areas of Al-Mg alloys. These alloys are used in construction of aircraft structures such as wings and fuselages. These alloys are used in marine, automotive and aviation due to their high strength to density ratio. All the above mentioned applications shows that there is a lot of research required in the area of the mechanical properties

enhancement of the Al-Mg alloys, which has led to the origin of this study. There is a possibility of study in the field of inter metallic layers temperature and heat distribution of weld joint and finite element analysis for better understanding the process. Further studies are possible for the cold spray coating which can increase the strength of joint. Further studies are possible in the field of simulation process. Studies are also possible in automatic sensor and control of process with the help of fuzzy logic and neural network approach. There are possibility of optimization of parameters by use of different optimization method like grey relational analysis, RSM method, neural network approach and fuzzy logic approach to decide the optimum parametric combination for best joint quality. Further studies are also possible post weld heat treatment of the joint to achieve the better mechanical strength of the joint.

Based on the scopes following objectives are chosen for our study

- Study the effect of MIG welding parameters on tensile strength, toughness and micro hardness behaviour at fusion and heat affected zone.
- Study the post weld aging effect on MIG welded Al alloy plates at different parameters level.
- Study the microstructural changes of MIG welded joint at fusion zone and heat affected zone.
- SEM analysis of fractured tensile and impact specimen.
- Optimization of welding parameter for the better mechanical properties of the welding joint by using Taguchi method
- Find out the best result from the different experiment trials by using Grey relation analysis.

CHAPTER-3

Material and Methodology

3.1 Introduction

This chapter describes the design of proposed work. It will include the overall objective of proposed work, the research methodology, basic information and concentrations regarding constituents of the proposed material, equipments and instruments required to study the welding of Al-Mg alloy.

3.2 Material

For the study of welding of Al-Mg alloy, work piece and electrode wire are the basic requirement. The selection of material and filler wire has been done based on past literature review, their applications and their technical specifications.

3.2.1 Work piece

Al-6063 has been selected as a work piece. It is the most common alloys of Aluminium which is used for general purpose. It contains 96-98% aluminium, 0.45-1.2% magnesium, silicon-0.2-0.6%, iron-0.10%, manganese – 0.1% etc. The density of the work piece is 2700 kg/m^3, melting point is 640° C. It is used for automotive parts and architecture parts like window frames and door frames. It has ultimate tensile strength of 250-320 MPa. After welding the properties of the alloy like ultimate strength reduces up to 35 percentages so it is recommended to post weld heat treatment so that properties of alloy can be improved.

3.2.2 Electrode Wire

In MIG welding there are different kinds of wire are used. But in this study, Aluminum wire of ER5356 grade has been taken. It is of 1.6 mm diameter. It has melting range of 600-680° C. It has excellent flow characteristics and penetration. It has excellent crack resistance. It is used for different automotive applications. It has a tensile strength of 120 MPa. For this Argon is recommended as a shielding gas.

3.3 Equipment and Methodology

In this section, methodology to do the work is explained briefly. For this analysis, Design of Experiment has been used.

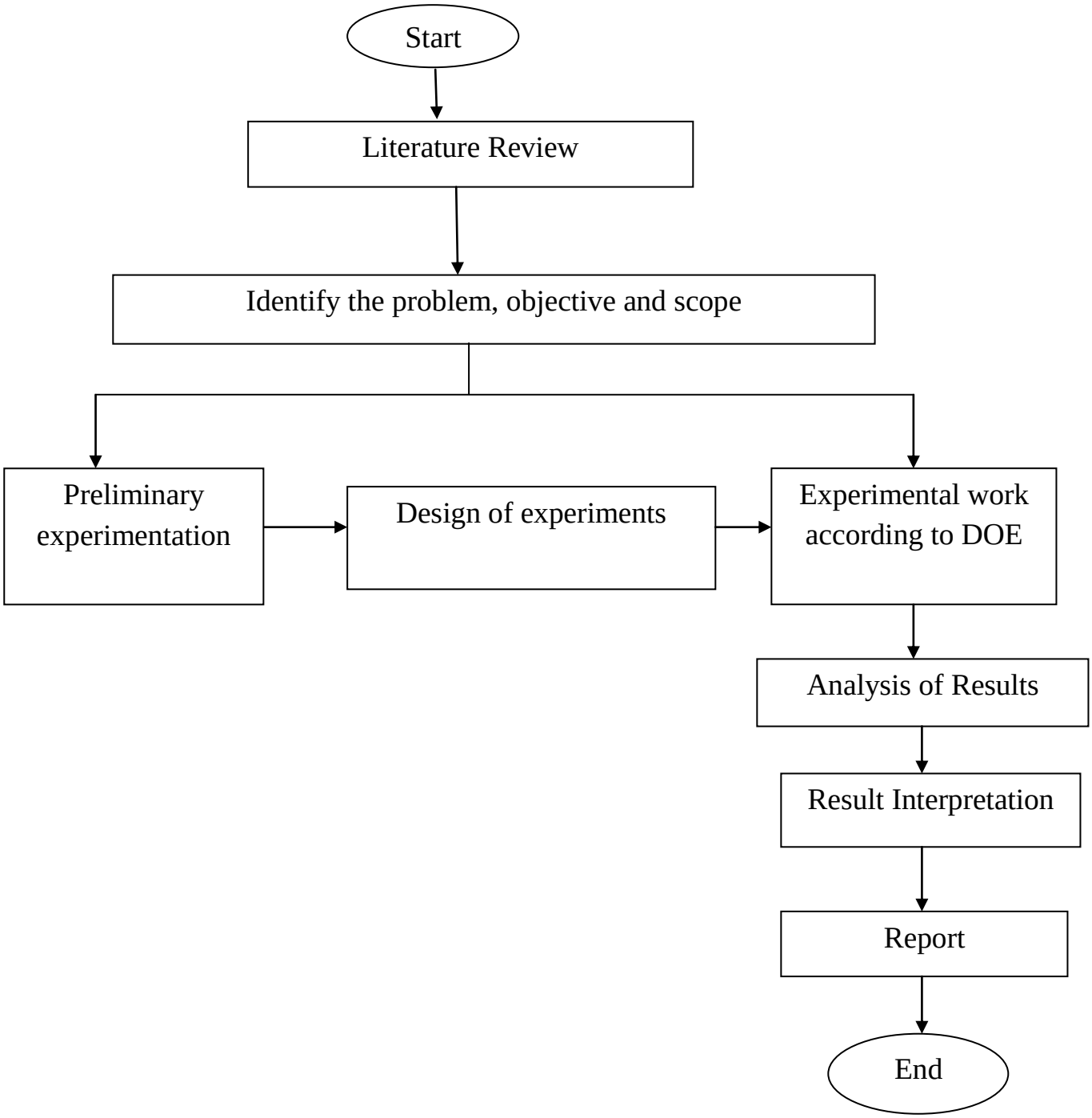

Fig 3.1: Flow chart of experimental work

3.3.1 Welding Machine

The experiments have been conducted on MIG welding machine which is available at Thapar University, Patiala in workshop lab as shown in Fig 3.1. It consists of different parts like transformer, pressure cylinder, spool wire, welding torch, nozzle etc. There is pressure cylinder which is connected by a flow regulator. The gas flow rate is set by this device. In this machine there is a separate regulator of current, voltage and arc force. Each parameter can be set to a definite value in every welding. Each parameter has its effect on the output parameters such as mechanical strength, microstructure, power and feed rate which will vary on experimentation. The ranges of the values of these parameters for the experimental work have been selected on the basis of some trial experiments for which certain quality factors are taken care. There is a wire feed mechanism attached to the machine.

Fig 3.2: MIG welding machine

3.3.2 Edge preparation

An Aluminum 6063 alloy plates of dimensions 100 mm x 80 mm x 6 mm was taken. After this, with the help of angle scale, plate is fixed on desk and filing is done on desired angle and up to desired position. Then it was completely washed with acetone so that there should not be any oxygen content in the plate. Oxygen content is the main problem in the welding of Al-Mg alloy. So it should be removed. Then a soft copper wire brush was use to make the plate oxide free. Thus the plates get ready for joint preparation.

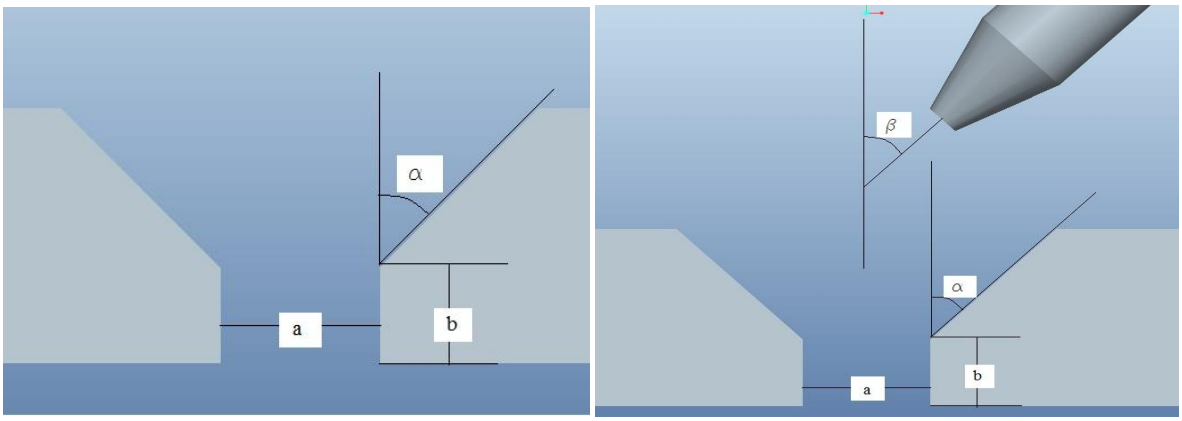

Fig 3.3: CAD model of joint preparation

3.3.3 Shielding gas

In Aluminum welding, there is a problem of oxide formation which reacts to the metal very easily. This is why we use inert gas for the welding of aluminum alloy. There are different inert gases. Helium, Argon and their mixture are commonly used as inert shielding gas flow protecting weld pool. The selection of inert gas to be used as shielding gas in MIG welding process depend upon type of metal to be welded. In our study, Argon has taken because it has some advantages. It has higher density so it has a higher flow rate. It has easy arc initiation. It provides good cleaning action with AC/DCEP in Al-Mg polarity. Pure argon gas produces shiner and clean weld surface compare to helium. Helium is used where a high penetration weld is required. In some case, mixtures of both gases are used.

3.3.4 Measuring equipments

- **Tensile Test (Universal Testing Machine):** The universal testing machine (TUE-C-1000-SERVO) is used to carry out the tensile tests of different materials. It has a capacity of 1000 kN, provided with different fixtures for tensile and flexural testing. This machine has maximum allowable elongation of 250 mm. It has electronically sophisticated imported pressure and flow control valve with dedicated controller which is used to provide desired loading and strain rate. The loads and strain rate are provided with computer attached to the machine. It has DAS panel with 32 bit micro controller system which can be connected to different computer systems. It has load accuracy as high as ± 1% of machine capacity. The machine satisfies IS: 1828 and BS: 1610 standards. It has accurate and user friendly software which provide accurate information and different plots like stress vs strain, load vs displacement graph. For this test, the sample is prepared according to ASTM standard. Before test is done, gauge length is marked in the specimen and measure the initial gauge length and diameter or width of the specimen. Then the tensile load is applied by the machine. The load is applied until the fracture happens. After fracture measure the maximum load, final gauge length and width of the specimen. With the help of maximum load, ultimate strength is calculated by dividing the load by initial cross section area. With the help of changing in gauge length, percentage elongation can be calculated.

Fig 3.4: Universal testing machine

(Photo courtesy: Mechanical Engineering Department, Shri Guru Granth Sahib World University, Patiala)

- **Metallurgical study:** For metallurgical study, different kinds of microscopes are used. The metallurgical and measuring microscopes are available in Mechanical Engineering department, Thapar University, Patiala. It magnifies the small images of sample. It is helpful in checking the metallurgical effect of welded samples. It has a camera attached to it which can take snapshots by enlarging the images. It has different lenses like 10x, 20x, 50x, 100x. It is attached with computer which shows the different views in a proper manner. In this, software is used to watch the images in computer screen. With the help of this software annotation can be done on the images. Besides this brightness of the image can also be adjusted. We can view the effect of different parameters of welding in this machine. It is helpful in predicting the behaviour of the surface.

Fig 3.5: Metallurgical Microscope

- **Microhardness**: Microhardness usually used for soft material or such material where we can not apply high load. The term Micro Hardness Testing usually refers to static indentations made by loads of 1kg or less. It is available in Mechanical department, Thapar University, Patiala. In this machine, we can vary load from 50 g to 1 Kg. The work piece which hardness is to be measured is put under microscope. Then load is applied to the work piece. There is a dwell time up to which indenter indent on the surface of work piece. The shape of the tool is square pyramidical and it is made of diamond. After the load is removed, the indentation is watched in the desktop attached to it. The camera attached to micro hardness machine helps in watching the indentation on the desktop. In the desktop, there is 'Quantimet' software which is used to calculate the harness value. First the software needs to be calibrated. The plate which hardness needs to be measured must be properly cleaned and polished so that there should not be any scratch on indentation. After calibration, load is defined in software and four ends of the square indentation are selected. The software automatically calculates the dimensions of indentation and corresponding Vickers hardness value.

Fig 3.6: Micro hardness Testing Machine

- **Charpy toughness test:** Toughness is defined as the energy absorption capacity of the material before its failure takes place. In stress curve, it is shown as the area under the curve. For brittle material, toughness value is low but for ductile material, toughness is high. For this test, a notch is provided in the metal. Specimen is placed on supports or anvil so that the blow of hammer is opposite to the notch. The material is placed at simple supported position in Charpy test and it is place such that when hammer strikes the work piece, it will generate tensile force in it. For Charpy impact test, the standard size of specimen is 55 x 10 x 10 mm. An indicator is attached to the machine which shows the reading of toughness in Joule. There is a scale for impact reading. The scale is 1 division equals to 2 Joule. The notch is provided in the specimen so that stress concentration value increases at that point and the specimen breaks from that point. In Charpy impact test, the height of the hammer striking is more as compare to Izod so Charpy consumes more energy as compare to Izod test.

Fig 3.7: Charpy toughness testing Machine

(Photo Courtesy: Mechanical Engineering department, Punjabi University, Patiala)

- **Scanning Electron Microscopy (SEM):** The scanning electron microscopy (SEM) is used to view the structure at different ranges. In this an electron beam is passed to the work piece then secondary electrons are emitted from the plate. Topography of the surface can be observed by electron probe over the surface and acquisition of an image from the detected secondary electrons. This SEM (Make: JSM-6510LV, JEOL Ltd, Tokyo, Japan) is available at SAI Labs, Thapar Technology Campus, Patiala. SEM analysis is a "non-destructive" test because the fine electron beam doesn't leads to the loss in the volume from the work piece surface. It is a high performance and low vacuum SEM for fast characterization and imaging of fine structures and has a magnification range 5–300,000 X. For this, a high vacuum is required, because electron should be focussed on the particular zone. So a high vacuum is created inside the box of the machine. This machine is connected with EDS in which phase composition can be watched.

Fig 3.8: Scanning electron microscope

3.3.5 Pilot Experimentation and selection of factors

In pilot study, different experiments were conducted at different parameter values to obtain the most satisfactory parameter value range. In this study, we have done pudding on Aluminium plate at different current values. The values of current at constant voltage 24 V were 150, 170, 190,210 Amp. It was done on the same plate at some distance. There was around one or two hour gap in next welding so that there should be no effect of heat parameter on the next welding. Similarly the same thing was done at different voltage. The different voltage values are 18, 20, 22, 24 V.

Fig 3.9: Base and pudding plate

After pudding, plate was cut from centre. Then it was cleaned with the help of hard file, smooth file and different emery papers. 600 and 800 number Emery paper was used to clean the surface. After this, Keller's etchant was used to see the effect of different parameters used on that plate. The composition of Keller's etchant has given in Table-3.1

Table 3.1: composition of Keller's etchant

Solution	Amount
Methanol	25 ml
Hydrochloric Acid	25 ml
Nitric Acid	25 ml
Hydrofluoric acid	1 drop

- **Results of Pilot experimentation:** After Keller's etchant was used, the surface looks as shown in Fig: 3.10.

(a)

(b)

Fig 3.10: Plate surface after etchant used

From the reviewed paper and after pilot experimentation, it was found that we get proper penetration shape at 170 and 190 Amp and we get optimal beading at 20 and 22 V. Besides this we also get the knowledge of other factor like groove angle, torch angle, gas flow rate, welding speed, filler material, electrode diameter and post weld treatment also affects the welding process. So these are the important factors which affect the welding process.

Selection of factors and their levels: With the help of literature reviews and pilot experimentation, selected factors are shown in Table 3.2

Table 3.2: parameters and their levels

S. no.	Parameter	Level
1	Current	150,170,190 A (3)
2	Voltage	20,22,24 V (3)
3	Groove Angle	60°,75°, 90° (3)
4	Gas flow rate	10,13,16 L/min (3)
5	Post weld aging	No, 160°C for 6 hours(2)

3.3.6 Selection of orthogonal array

After selection of parameters and their levels, there should be proper selection of orthogonal array. For this, proper knowledge of design of experiments is necessary. Design of Experiments is widely used in research and engineering problems where the different number of factor requires optimization. This method requires very less cost because in this few numbers of experiments are required to perform. DOE requires only a small set of experiments and thus helps to reduce costs. There are many types of design of experiments applied in research and development but out of which the most common and efficient method is Taguchi method that is used for the optimization process of various parameters. The selection of orthogonal array depends upon the factors and their levels. Suppose if there are all the factors of 2 levels then L4, L8, L16, L32, L64 etc. can be applied. If all the factors of 3 levels then L9, L27, L81 can be used. If some factors are of 2 level and some are of 3 levels then we can use L6, L12, and L18 etc. The selection of orthogonal array is based on the fact that total degree of freedom of selected factor should be less or equal to the degree of freedom of selected array.

In this work, some factors are of 2 level and some are of 3 levels. So mixed level orthogonal array L18 has been used. Orthogonal array L18 has been shown in Table 3.3. In this total number of the experiment are 18. This is the advantage of using orthogonal array because it reduces the number of experiment.

Table 3.3: Orthogonal array (L18)

S.No.	Pose weld Aging	Current (A)	Voltage (V)	Gas flow rate (L/min)	Groove Angle (Degree)
1	No	150	20	10	60
2	No	150	22	13	75
3	No	150	24	16	90
4	No	170	20	10	75
5	No	170	22	13	90
6	No	170	24	16	60
7	No	190	20	13	60
8	No	190	22	16	75
9	No	190	24	10	90
10	180° C, 6 hour	150	20	16	90
11	180° C, 6 hour	150	22	10	60
12	180° C, 6 hour	150	24	13	75
13	180° C, 6 hour	170	20	13	90
14	180° C, 6 hour	170	22	16	60
15	180° C, 6 hour	170	24	10	75
16	180° C, 6 hour	190	20	16	75
17	180° C, 6 hour	190	22	10	90
18	180° C, 6 hour	190	24	13	60

For our problem, L18 has been taken which has a 17 degree of freedom. Each column has one degree of freedom. So there should be 17 columns. In this analysis there are 5 factors in which four factors have 3 level parameters and one factor has 2 level parameter. So there are 4 column of 2 degree of freedom and one column has one degree of freedom. So these 5 columns show the 9 degree of freedom. Since L18 has 17 degree of freedom and only 5 columns are assigned which has 9 degree of column so the rest column will show the error

which has 8 degree of freedom. Error study is done because it is helpful in determining the ANOVA table.

3.3.7 Signal to noise ratio for response characteristics

After selection of array, we need to find the signal to noise ratio. Basically factors can be categorized of 2 types. One is controllable factor (signal) which can be easily adjusted by designer. Second is uncontrollable factor (noise) which is the sources of variation associated with environment. The change in desired quality with respect to controllable factor is called the signal while the effect of uncontrollable factor is termed as noise. The objective of the work is to find out the proper signal to noise ratio.

So we need to understand the objective of our work. Depending upon the type of response, there are 3 types of signal to noise ratio.

- **Higher the better**

$(S/N)_{HB}$ = -10 log $(MSD)_{HB}$ where

$$MSD_{HB} = \frac{1}{R}\sum_{j=1}^{R}\frac{1}{y_j^2}$$

MSD_{HB} = Mean square deviation for higher the better response

- **Lower the better**

$(S/N)_{LB}$ = -10 log $(MSD)_{LB}$

$(MSD)_{LB} = \sum_{j=1}^{R} y_j^2$

$(MSD)_{LB}$ = Mean square deviation of lower the better response

- **Nominal the better**

$(S/N)_{NB}$ = -10 log $(MSD)_{NB}$

$(MSD)_{NB} = \frac{1}{R}\sum_{j=1}^{R}(y_j - y_o)^2$

$(MSD)_{NB}$ = Mean square deviation of nominal the better response

Y_j = observed value of response characteristics

Y_o = Nominal value of results

R = Number of repetitions

3.3.8 Grey Relational Analysis

Grey relational analysis is used to find the optimal result from the given trial conditions. It is used when there are different response quality parameters. This methodology converts the different objective quality parameters into single objective quality parameter. This methodology converts the different responses into single grey grade. The grey relational grade which has maximum value is the optimal result for different responses.

3.3.9 Experimental Work

In this aluminum plates were cleaned by acetone. Then they were clamped into fixture and tacking was done on both ends of the plate. Then plates were welded at different parameters according to orthogonal array. The tacking plates and welded plates are shown in Fig 3.11.

Fig 3.11: Tacking and weld plates

In orthogonal array, some plates required post weld aging process. So after welding they were kept in oven at 180̊ C for 6 hours and after that they were cooled in the oven at room temperature. After this process tensile test specimen, impact test specimen, micro hardness specimen and metallurgical testing specimen were cut from the plate.

- **Preparation of tensile test specimen**

The dimensions of tensile test specimen were decided according to ASTM standard E8M-04. All the dimensions are shown in Fig 3.12. All the dimensions shown in the figure are in mm.

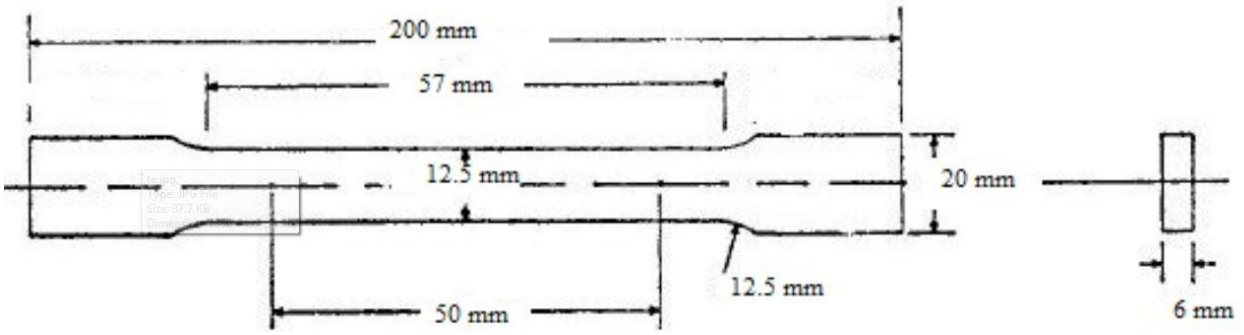

Fig 3.12: CAD model of tensile test specimen

For preparation of tensile test specimen, first 20 mm width specimen was cut from the welded joint. Then with the help of end milling cutter and milling machine as shown in Fig 3.13, required dimensions were achieved in the plate.

Fig 3.13: Milling Machine

After this the specimen is filed and grinded to remove the undesired chips remaining on the plate. Thus the final tensile test specimen was prepared. The final tensile test specimen is shown in Fig 3.14.

Fig 3.14: Tensile specimen

- **Preparation of Charpy toughness specimen**

The dimension of the Charpy impact test specimen is 55 x 10 x 10 mm. There is a V notch of 2 mm depth at 45 degree angle. First the plate was cut in required dimensions. Then notch is provided by shaper. The shaper tool is made at 45 degree angle. The Charpy toughness specimen has been shown in Fig 3.15

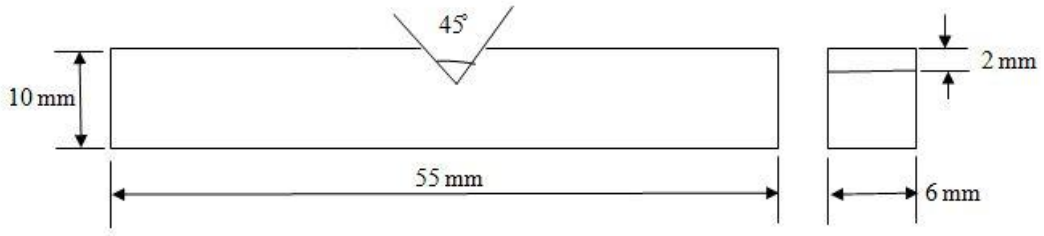

Fig 3.15: Charpy toughness specimen

Preparation of micro hardness and metallurgical specimen

These samples were prepared by Filing and polishing of specimen by different emery paper grade. After polishing, specimens were etched by Keller's etchant so that both fusion zone and heat affected zone can be viewed easily.

After preparation of all samples, testing was done on it.

CHAPTER 4

Results and Discussions

4.1 Introduction

This chapter includes the results of experiments performed on MIG welded aluminium alloys plates along with the interpretation. The objective of the study to determine the effect of welding parameters like current, voltage, gas flow rate, the effect of groove angle and post weld aging on the mechanical properties like tensile strength, toughness, micro hardness and metallurgical effect of welded joint. Signal to noise ratio was also determined and graphs were plotted on the basis of experimental data and analyzed it from the results. For graphical analysis of the experimental results plots, showing effect of all the factors upon responses, are generated in MINITAB. Then ANOVA of the experimental data has been used to find the significance of each factor for every output responses like tensile strength, impact strength and micro hardness. After studying the effect of all factors individually, signal to noise ratio was also calculated. For tensile strength and impact strength higher the best approach is used and for micro hardness nominal is better approach is used. After this, optimal solutions have been calculated for every response like tensile strength, impact strength and micro hardness.

4.2 Tensile strength

The various responses of tensile strength at different level has been shown in Table 4.1

Table 4.1: Various responses of tensile strength

S.No.	Post weld aging	Current (A)	Voltage (V)	Gas flow rate (L/min)	Groove angle (degree)	Tensile strength (MPa)
1.	No	150	20	10	60	168
2.	No	150	22	13	75	122.8
3.	No	150	24	16	90	158.467
4.	No	170	20	10	75	151.067
5.	No	170	22	13	90	166.133
6.	No	170	24	16	60	165.867
7.	No	190	20	13	60	152.933
8.	No	190	22	16	75	138
9.	No	190	24	10	90	142.667
10.	180̊ C,6 hour	150	20	16	90	187.067
11.	180̊ C,6 hour	150	22	10	60	142.933
12.	180̊ C,6 hour	150	24	13	75	168
13.	180̊ C,6 hour	170	20	13	90	205.6
14.	180̊ C,6 hour	170	22	16	60	173.067
15.	180̊ C,6 hour	170	24	10	75	154.933
16.	180̊ C,6 hour	190	20	16	75	168.073
17.	180̊ C,6 hour	190	22	10	90	147.067
18.	180̊ C,6 hour	190	24	13	60	173.2

With the help of these responses, graphs are plotted in MINITAB. Fig 4.1 shows the effect of different parameter on tensile strength.

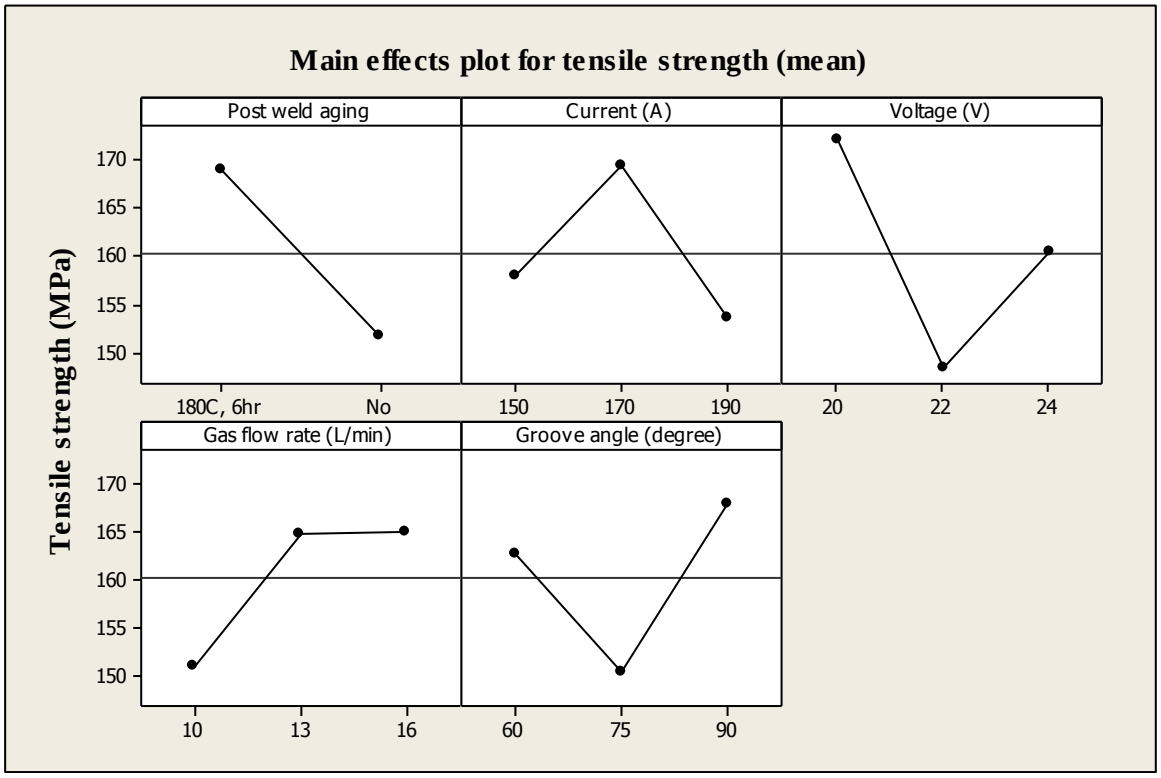

Fig 4.1: Effect of various factors on Tensile strength

Fig 4.1 shows the effect of different welding parameters on the tensile strength of the joint. The tensile strength of the base metal is high as comparison to weld metal and post weld heat treated plate because on welding, brittleness of the plate increases. From Fig 4.1 it is clear that post weld aging effect increase the tensile strength of weld joint. This happens because post weld aging increases the ductility of joint which affect the tensile strength. Graph shows that on increasing the current, tensile strength first increases then decreases. This is because on increasing current penetration increases. Thus filling of filler material fills in the joint properly but excessive current can distort the plate. Thus tensile strength decreases. On increasing the voltage, weld bead increases but excessive bead decreases the tensile strength of weld. Thus result shows that on increasing the voltage, tensile strength decreases. The result shows that on increasing gas flow rate, tensile strength increases.

Table 4.2: ANOVA table of tensile strength

Source	DF	Sum of square	Variance	$F_{Calculate}$	F_{Table}	Significance
Post weld aging	1	1317.7	1317.66	15.74	5.32	Significant
Current	2	801.7	400.86	4.79	4.46	Significant
Voltage	2	1698.2	849.12	10.14	4.46	Significant
Gas flow rate	2	764.6	382.28	4.57	4.46	Significant
Groove angle	2	952.8	476.42	5.69	4.46	Significant
Error	8	669.8	83.73			
Total	17	6204.8				

From the ANOVA Table 4.2, it is clear that every parameter is significant for tensile strength because for every parameter, F value is greater than F critical values of table at 95% confidence interval. From the results, it is clear that post weld aging increases the tensile strength of the weld joint. Other welding parameters like current, voltage, gas flow rate and groove angle also affect the tensile strength of the joint.

Table 4.3: Response table for tensile strength

Level	Post weld aging (*A*)	Current (*B*)	Voltage (*C*)	Gas flow rate (*D*)	Groove angle (*E*)
1	168.9	157.9	172.1	151.1	162.7
2	151.8	169.4	148.3	164.8	150.5
3		153.7	160.5	165.1	167.8
Delta	17.1	15.8	23.8	14	17.4
Rank	3	4	1	5	2

From Table 4.3, it is found that maximum value of delta is 23.8 which come in voltage. So voltage is the most significant factor for tensile strength in this experimental setup. From the Table 4.3, it is found that optimum combination for tensile strength is $A_2B_2C_1D_3E_3$. So the optimal solution of mean of tensile strength of this experimental setup has been calculated.

$\mu_{opt} = \bar{m} + (m_{A2} - \bar{m}) + (m_{B2} - \bar{m}) + (m_{C1} - \bar{m}) + (m_{D3} - \bar{m}) + (m_{E3} - \bar{m})$

$= 160.3 + (168.9-160.3) + (169.4-160.3) + (165.1-160.3) + (167.8-160.3)$

$= 190.3$ MPa

Here μ_{opt} = desired mean value

Confidence interval has also been calculated for this experimental work.

$$CI = \sqrt{\frac{F_{\alpha,v1,v2}V_e}{n_{eff}}}$$

Where $F_{\alpha, v1, v2}$ = F ratio

$\alpha = 0.05$ (risk level)

v_1 = degree of freedom for mean (always 1)

v_2 = Total degree of freedom = 17

$\bar{m}$ = average of all experiment trial

$$n_{eff} = \frac{N}{1 + DF_{A,B,C,D,E}}$$

n_{eff} = number of tests under that condition using the participating factors

N = number of trial in the experiment

$n_{eff} = \frac{18}{1+9} = 1.8$

Here V_e = Variance of error

$CI = \sqrt{\frac{4.45 \times 83.73}{1.8}} = \pm 14.39$

Thus the optimal value for tensile strength is 190.3 ± 14.39.

4.3 Toughness

The various responses of toughness, their mean value and SN ratio are shown in Table 4.4

Table 4.4: Responses of toughness at different experimental trials

S.No.	Toughness (J)		Mean toughness (J)	SN ratio
	Reading 1	Reading 2		
1	4	4	4	12.04
2	2	4	3	8.061
3	4	6	5	13.45
4	4	4	4	12.04
5	8	6	7	16.64
6	10	8	9	18.92
7	8	6	7	16.64
8	4	2	3	8.06
9	4	4	4	12.04
10	8	10	9	18.92
11	6	4	5	13.45
12	8	8	8	18.06
13	12	10	11	20.72
14	14	12	13	22.20
15	6	8	7	16.64
16	6	6	6	15.56
17	4	4	4	12.04
18	10	8	9	18.92

(Refer Table 3.3 for experimental trials)

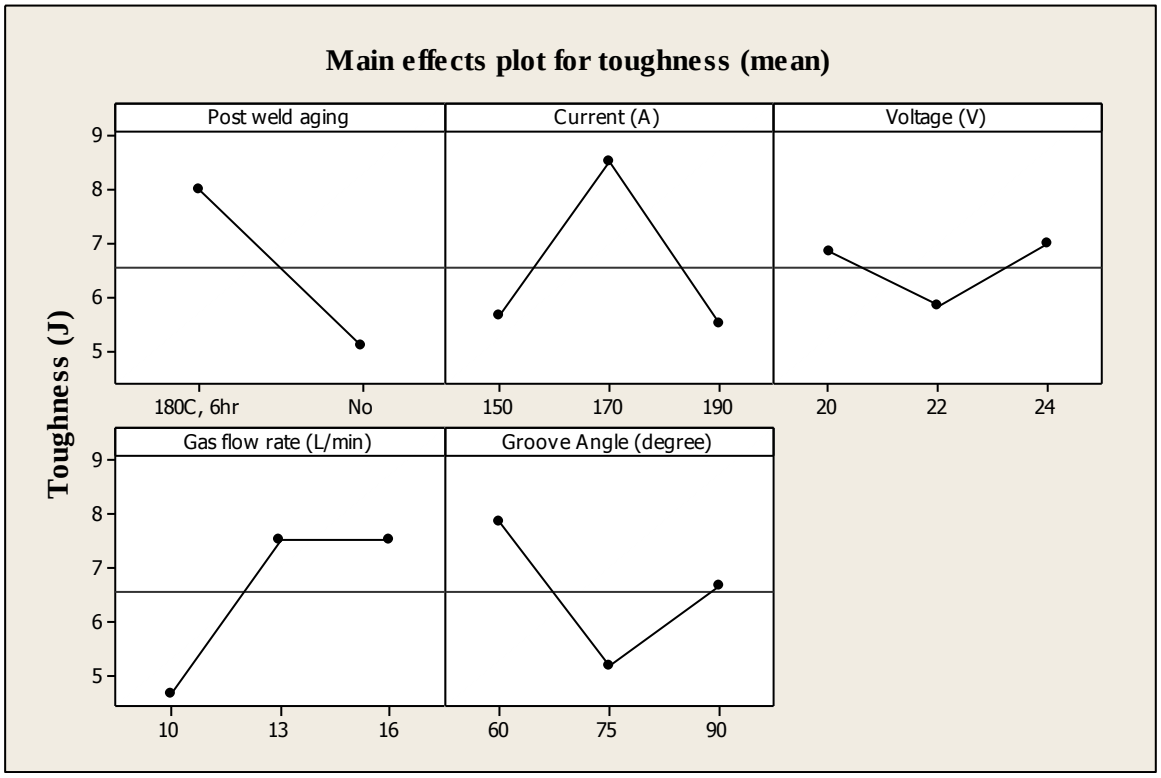

Fig 4.2: Effect of various factors on toughness

From Fig 4.2, it is clear that post weld aging increases the toughness of the weld specimen. As the current increases, the rate of penetration increases. Thus toughness increases. But after a certain level, excessive current leads to distort the joint which affect the toughness of the joint. From the results, it is clear that on increasing the voltage, toughness decreases. This happens because on increasing the voltage, size of weld bead increases which means heat input increases. As heat input increases, toughness decreases. Graph shows that as gas flow rate increase, toughness increases because gas flow rate controls the heat input rate which affects the impact energy of joint. On increasing the groove angle, toughness decreases.

.

Table 4.5: ANOVA table for toughness (mean)

Source	DF	Sum of square	Variance	$F_{Calculate}$	F_{Table}	Significance
Post weld aging	1	37.556	37.556	35.58	5.32	Significant
Current	2	34.111	17.056	16.16	4.46	Significant
Voltage	2	4.778	2.389	2.26	4.46	Not Significant
Gas flow rate	2	32.111	16.056	15.21	4.46	Significant
Groove angle	2	21.444	10.722	10.16	4.46	Significant
Error	8	8.444	1.056			
Total	17	138.444				

From Table 4.5, it is clear that post weld aging, current, gas flow rate and groove angle are significant. But the voltage is not significant for toughness for mean values of toughness.

Table 4.6: Response table for toughness

Level	Post weld aging (*A*)	Current (*B*)	Voltage (*C*)	Gas flow rate (*D*)	Groove angle (*E*)
1	8	5.667	6.833	4.667	7.883
2	5.111	8.5	5.833	7.5	5.167
3		5.5	7	7.45	6.667
Delta	2.889	3	1.167	2.833	2.667
Rank	2	1	5	3	4

From Table 4.6, it is found that maximum value of delta is 3 which come for voltage. So voltage is the most significant factor for tensile strength in this experimental setup. Table 4.6 shows the average values of toughness at different level. For Higher the better condition, the optimum condition for this experimental set up is $A_2B_2D_2E_1$. So the optimal solution has been calculated.

$\mu_{opt} = \bar{m} + (m_{A2} - \bar{m}) + (m_{B2} - \bar{m}) + (m_{D2} - \bar{m}) + (m_{E1} - \bar{m})$

$= 6.556 + (8-6.556) + (8.5-6.556) + (7.5-6.556) + (7.883-6.556)$

$= 12.215$

Here μ_{opt} = desired mean value

Confidence interval has also been calculated for this experimental work.

$$CI = \sqrt{\frac{F_{\alpha,v1,v2}V_e}{n_{eff}}}$$

Where $F_{\alpha, v1, v2}$ = F ratio

$\alpha = 0.05$ (risk level)

v_1 = Degree of freedom for mean (always 1)

v_2 = Total degree of freedom = 17

$\bar{m}$ = average of all experiment trial

$$n_{eff} = \frac{N}{1 + DF_{A,B,D,E}}$$

n_{eff} = number of tests under that condition using the participating factors

N = number of trial in the experiment

$n_{eff} = \frac{18}{1+7} = 2.25$

Here V_e = Variance of error

$CI = \sqrt{\frac{4.45 \times 1.056}{2.25}} = \pm 1.45$

Thus the optimal solution for this experimental set up is 12.215 ±1.45 J.

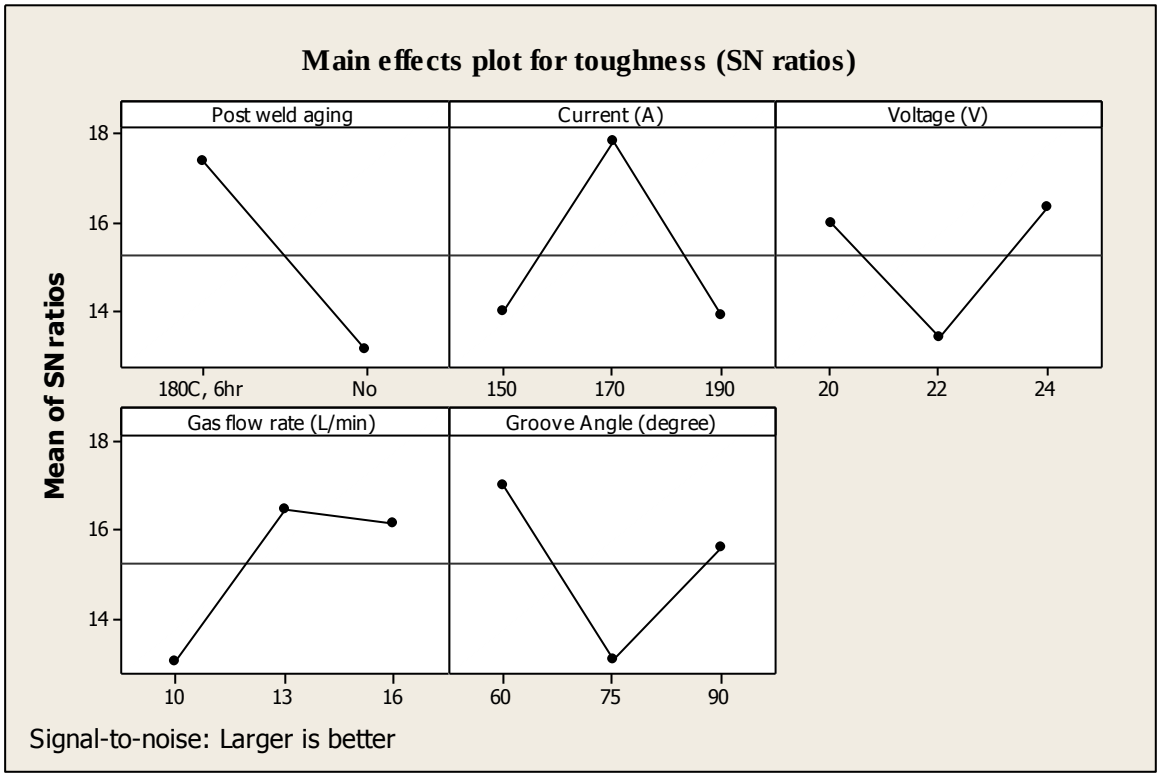

Fig 4.3: SN ratio curve for toughness

Fig 4.3 shows the signal to noise variation for toughness. The plot shows the same effect which was found for mean results. It shows that post weld aging increases the toughness of weld joint. This figure confirms that parameters of same level give the desired output.

Table 4.7: ANOVA table for toughness (SN ratios)

Source	DF	Sum of square	Variance	$F_{Calculate}$	F_{Table}	Significance
Post weld aging	1	82.90	82.90	41.64	5.32	Significant
Current	2	61.54	30.77	15.46	4.46	Significant
Voltage	2	30.72	15.36	7.72	4.46	Significant
Gas flow rate	2	43.99	21.995	11.05	4.46	Significant
Groove angle	2	48.40	24.2	12.16	4.46	Significant
Error	8	15.93	1.991			
Total	17	283.47				

Table 4.7 shows the ANOVA table for SN ratio variation. It shows that voltage is also a significant factor for toughness. There is a great effect of voltage on toughness. On increasing

voltage, toughness decreases because on increasing voltage, heat input increases which decrease the toughness value.

4.4 Fusion zone microhardness

Fusion zone is the zone where weld metal flows in the plate. In this zone melting, solidification and micro structural change takes place. The various responses of microhardness in fusion zone have been shown in Table 4.8.

Table 4.8: Various responses of fusion zone microhardness at different experiments trials

S.No.	Fusion zone microhardness (VHN)			Mean microhardness (VHN)	SN ratios
	Reading 1	Reading 2	Reading 3		
1	94.817	96.896	97.251	96.32133	37.3
2	117.2164	115.6154	112.3854	115.0724	33.4
3	97.217	99.948	98.51962	98.56154	37.17
4	98.682	95.5695	92.269	95.50683	29.48
5	90.26614	91.25099	95.15646	92.22453	31.04
6	91.354	92.27586	93.27586	92.30191	39.65
7	99.25408	97.53285	93.27586	96.6876	36.3
8	104.268	105.893	107.5147	105.8919	36.29
9	92.561	90.746	90.367	91.22467	37.82
10	84.011	86.686	82.368	84.355	31.76
11	101.1038	103.3066	104.248	102.8861	36.09
12	90.237	85.265	88.968	88.15667	30.66
13	80.238	78.478	79.354	79.35667	39.1
14	82.5678	81.3275	84.527	82.80743	34.21
15	81.90509	84.8104	83.578	83.43116	35.15
16	87.55946	85.377	84.542	85.82615	34.82
17	90.15387	85.645	88.107	87.96862	31.81
18	82.822	84.966	86.149	84.64567	34.01

(Refer Table 3.3 for experiments trials)

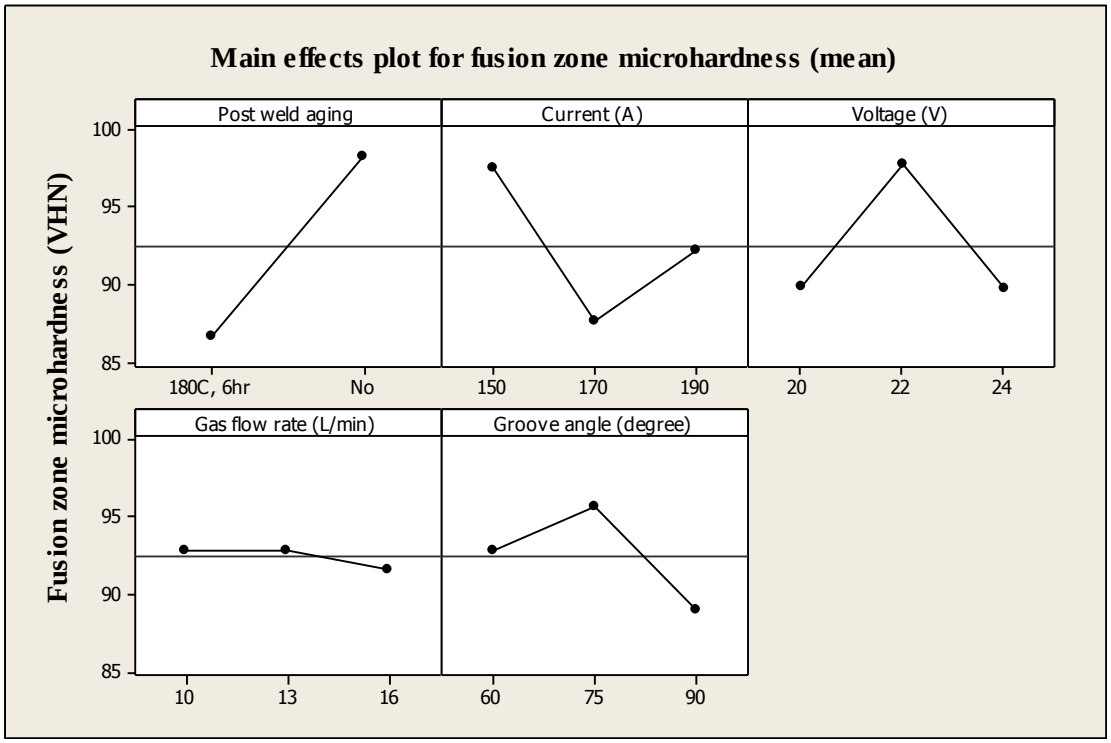

Fig 4.4: Effect of various factors on Micro hardness in FZ (mean)

From Fig 4.4, it is clear that post weld aging reduces the micro hardness of the joint because it increases the ductility of the material. On increasing current, first micro hardness reduces and then micro hardness increases. This happens because on increasing current first ductility increases and then ductility reduces. And on increasing the voltage, micro hardness increases because voltage increases the brittleness of the material. There is no effect of gas flow rate on micro hardness.

Table 4.9: ANOVA table for fusion zone microhardness

Source	DF	Sum of square	Variance	$F_{Calculate}$	F_{Table}	Significance
Post weld aging	1	616.7	616.7	37.72	5.32	Significant
Current	2	297.81	148.905	8.99	4.46	Significant
Voltage	2	257.78	128.892	7.78	4.46	Significant
Gas flow rate	2	6.25	3.125	0.19	4.46	Not Significant
Groove angle	2	135.54	67.77	4.06	4.46	Not Significant
Error	8	132.55	16.569			
Total	17	1446.63				

From the ANOVA table, it is clear that post weld aging; current and voltage have significant effect for micro hardness in fusion zone. Gas flow rate does not have effect. Groove angle has significant effect on hardness at 90% confidence interval but it does not have significant affect at 95% confidence interval.

Table 4.10: Response table for fusion zone microhardness

Level	Post weld aging (*A*)	Current (*B*)	Voltage (*C*)	Gas flow rate (*D*)	Groove angle (*E*)
1	86.6	97.56	89.84	92.89	92.78
2	98.31	87.6	97.81	92.86	95.65
3		92.21	89.72	91.62	88.95
Delta	11.71	9.95	8.09	1.27	6.70
Rank	1	2	3	5	4

From Table 4.10, it is clear that post weld aging has highest delta value so it is most significant factor for fusion zone microhardness for this experimental setup. Table 4.10 shows the average values of microhardness at different level. For Nominal the better condition, the optimum condition for this experimental set up is $A_1B_3C_1$. So the optimal solution has been calculated.

$\mu_{opt} = \bar{m} + (m_{A1} - \bar{m}) + (m_{B3} - \bar{m}) + (m_{C1} - \bar{m})$

$= 92.46 + (86.6-92.46) + (92.21-92.46) + (89.84-92.46)$

$= 83.73$

Here μ_{opt} = desired mean value

Confidence interval has also been calculated for this experimental work.

$$CI = \sqrt{\frac{F_{\alpha,v1,v2} V_e}{n_{eff}}}$$

Where $F_{\alpha, v1, v2}$ = F ratio

$\alpha = 0.05$ (risk level)

v_1 = Degree of freedom for mean (always 1)

v_2 = Total Degree of freedom = 17

$\bar{m}$ = average of all experiment trial

$$n_{eff} = \frac{N}{1 + DF_{A,B,C}}$$

n_{eff} = number of tests under that condition using the participating factors

N = number of trial in the experiment

$n_{eff} = \frac{18}{1+5} = 3$

Here V_e = Variance of error

$CI = \sqrt{\frac{4.45 \times 16.569}{3}} = \pm 4.96$

Thus the optimal solution for this experimental set up is 83.73 ± 4.96 VHN.

4.5 Heat affected zone microhardness

Heat affected zone is that part of metal which also get affected by the weld of metal. The various responses of microhardness in heat affected zone have been shown in Table 4.11.

Table 4.11: Various responses of heat affected zone microhardness at different trials

S.No.	HAZ microhardness (VHN)			Mean microhardness (VHN)	SN ratios
	Reading 1	Reading 2	Reading 3		
1	74.3652	73.3269	76.35654	74.68	33.71
2	88.9862	89.3654	89.9862	89.45	44.97
3	77.2031	79.3652	78.6945	78.42	37
4	78.1201	75.3069	77.3216	76.92	34.49
5	70.2069	71.2776	72.1456	71.21	37.31
6	71.2108	73.9998	72.6932	72.63	34.33
7	77.897	76.3697	75.2315	76.5	35.15
8	81.2354	83.2561	82.6547	82.38	38
9	72.3698	70.7361	72.0036	71.7	38.45
10	64.2318	66.2003	65.2589	65.23	36.42
11	78.3254	75.2109	77.3621	76.97	33.67
12	71.5214	68.2359	70.3625	70.04	32.47
13	58.3654	60.1412	61.2354	59.91	32.33
14	62.3208	61.2386	60.5648	61.37	36.81
15	63.8745	61.4812	62.3251	62.56	34.24
16	67.2014	65.3047	65.2147	65.91	35.38
17	70.0102	68.2031	69.2358	69.15	37.65
18	62.3241	64.2358	63.2147	63.26	36.41

(Refer Table 3.3 for experiment trials)

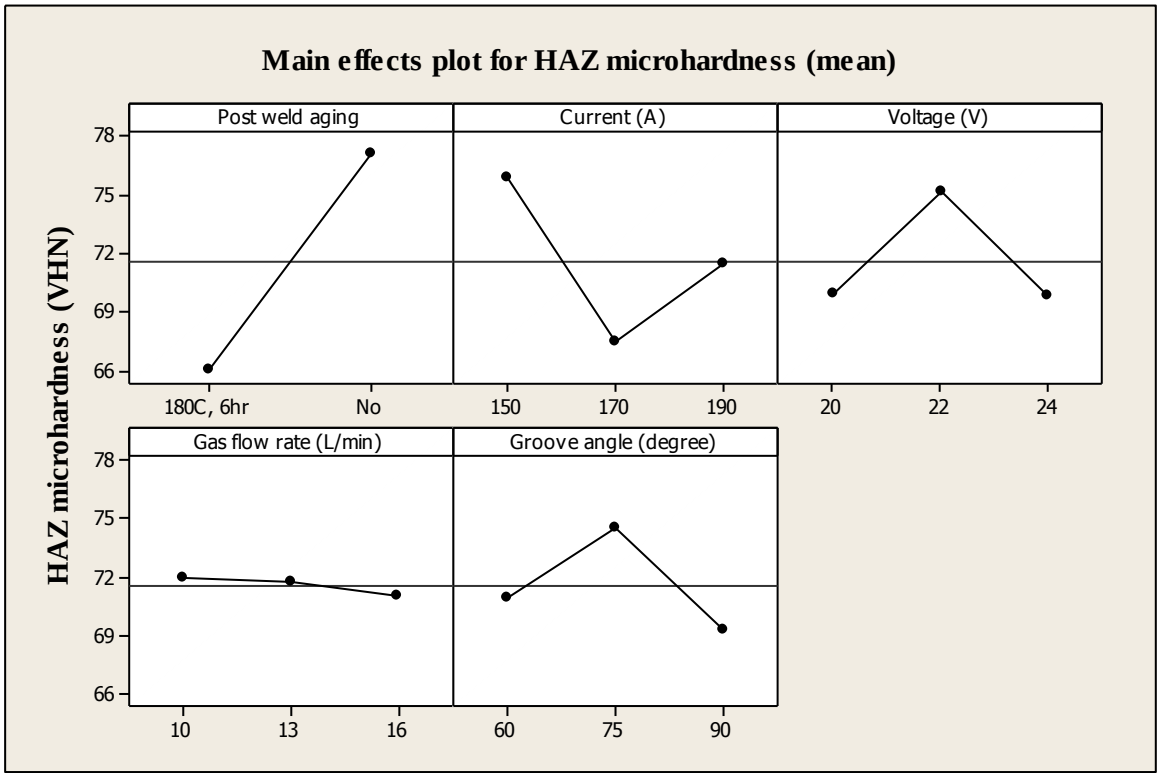

Fig 4.5: Effect of various factors on HAZ microhardness

From Fig 4.6, it is clear that post weld aging reduces the micro hardness of the joint because it increases the ductility of the material. On increasing current, micro hardness reduces. And on increasing the voltage, micro hardness increases because voltage increases the brittleness of the material. There is no effect of gas flow rate on micro hardness.

Table 4.12: ANOVA table for microhardness in HAZ (mean)

Source	DF	Sum of square	Variance	$F_{Calculate}$	F_{Table}	Significance
Post weld aging	1	549.96	549.96	51.68	5.32	Significant
Current	2	209.88	104.938	9.86	4.46	Significant
Voltage	2	111.29	55.646	5.23	4.46	Significant
Gas flow rate	2	3.25	1.624	0.15	4.46	Not significant
Groove angle	2	87.37	43.684	4.10	4.46	Not Significant
Error	8	85.14	10.643			
Total	17	1046.88				

From the ANOVA table, it is clear that post weld aging; current and voltage have significant affect for micro hardness in fusion zone. Gas flow rate does not have effect. Groove angle has

significant effect on hardness at 90% confidence interval but it does not have significant affect at 95% confidence interval.

Table 4.13: Response table for HAZ microhardness

Level	Post weld aging (*A*)	Current (*B*)	Voltage (*C*)	Gas flow rate (*D*)	Groove angle (*E*)
1	66.04	75.80	69.86	72	70.9
2	77.10	67.43	75.09	71.73	74.54
3		71.48	69.77	70.99	69.27
Delta	11.05	8.36	5.32	1.01	5.27
Rank	1	2	3	5	4

Table 4.14 shows that maximum value of delta comes for post weld aging. This signifies that post weld aging has highest effect on microhardness. Table 4.14 shows the average values of microhardness at different level. For Nominal the better condition, the optimum condition for this experimental set up is $A_2B_3C_1$. So the optimal solution has been calculated.

$\mu_{opt} = \bar{m} + (m_{A1} - \bar{m}) + (m_{B3} - \bar{m}) + (m_{C1} - \bar{m})$

$= 71.57 + (66.04-71.57) + (71.48-71.57) + (69.86-71.57)$

$= 64.24$

Here μ_{opt} = desired mean value

Confidence interval has also been calculated for this experimental work.

$$CI = \sqrt{\frac{F_{\alpha,v1,v2}V_e}{n_{eff}}}$$

Where $F_{\alpha, v1, v2}$ = F ratio

$\alpha = 0.05$ (risk level)

v_1 = Degree of freedom for mean (always 1)

v_2 = Total Degree of freedom = 17

$\bar{m}$ = average of all experiment trial

$$n_{eff} = \frac{N}{1 + DF_{A,B,C}}$$

n_{eff} = number of tests under that condition using the participating factors

N = number of trial in the experiment

$n_{eff} = \frac{18}{1+5} = 3$

Here V_e = Variance of error

$CI = \sqrt{\frac{4.45 \times 10.643}{3}} = \pm 3.97$

Thus the optimal solution for this experimental set up is 64.24 ± 3.97 VHN.

4.6 Multi-response optimization by using Grey Relational Analysis

Multi-response optimization techniques are used where different response or outcomes of a particular sample at same input parameter level are known. There are different methods of multi-response optimization technique like fuzzy logic, grey relation analysis etc. Grey relation analysis is used in this study.

4.6.1 Grey relation analysis

Grey relational analysis is used to find the optimal result from the given trial conditions. It is used when there are different response quality parameters. This methodology converts the different objective quality parameters into single objective quality parameter. This methodology converts the different responses into single grey grade. The grey relational grade which has maximum value is the optimal result for different responses.

The following steps are used in grey relational analysis.

1. Find out the experimental results of DOE.
2. Normalize the results in the domain of (0, 1) by using (a) and (b) equation.

- For higher the better result

$$N_{ij} = [X_{ij} - (X_{ij})_{min}] / [(X_{ij})_{max} - (X_{ij})_{min}] \ldots\ldots\ldots\ldots\ldots\ldots \text{(a)}$$

- For lower the better result

$$N_{ij} = [(X_{ij})_{max} - X_{ij}] / [(X_{ij})_{max} - (X_{ij})_{min}] \ldots\ldots\ldots\ldots\ldots\ldots \text{(b)}$$

Where N_{ij} = normalized value

$(X_{ij})_{max}$ = maximum value of response parameter

$(X_{ij})_{min}$ = minimum value of response parameter

X_{ij} = value of response in i column and j row matrix

3. Calculate $\Delta_{ij} = \left| N_{oj} - N_{ij} \right|$

   Where Δ_{ij} is the absolute value of difference in N_{oj} and N_{ij}

4. Calculate grey relation co- efficient by using equation (c)

$$Y\left(X_{oj}, X_{ij}\right) = \frac{\Delta_{min} + \varepsilon \Delta_{max}}{\Delta_{ij} + \varepsilon \Delta_{maxj}}$$

   Where Y = grey relation co-efficient

   ε = distinguish factor between 0 and 1. Here it is taken as 0.5

5. After calculating grey relation co- efficient, calculate grey relational grade by taking the average value of grey co- efficient.

4.6.2 Implementation of Grey analysis

Step 1: Results of tensile strength, toughness and microhardness are obtained for the trial conditions mentioned in Table 3.3 has been shown in Table 4.14.

Table 4.14: Various responses for trial conditions

S.No.	Tensile strength (MPa)	Toughness (J) (mean value)	Microhardness (VHN) (mean value)
1	168	4	96.32
2	122.8	3	115.07
3	158.467	5	98.56
4	151.067	4	95.51
5	166.133	7	92.22
6	165.867	9	92.3
7	152.933	7	97.69
8	138	3	105.89
9	142.667	4	91.23
10	187.067	9	84.36
11	142.933	5	102.89
12	168	8	88.16
13	205.6	11	79.36
14	173.067	13	82.81
15	154.933	7	83.43
16	168.073	6	85.83
17	147.067	4	87.97
18	173.2	9	84.65

(Refer Table 3.3 for trial conditions)

Step 2: Normalization (N) of various responses are shown in Table 4.15. The formulas are used as mentioned in 4.6.1. For tensile strength and toughness ‘Higher the better’ condition is used. For microhardness ‘Nominal the better’ condition is used. The nominal value is the microhardness value of base metal.

Table 4.15: Normalization table for various responses

S.No.	N for tensile strength	N for toughness	N for microhardness
1	0.5459	0.1	0.3745
2	0	0	0
3	0.4308	0.2	0.3297
4	0.3414	0.1	0.3907
5	0.5233	0.4	0.4563
6	0.5201	0.6	0.4548
7	0.3639	0.4	0.3672
8	0.1836	0	0.1833
9	0.2339	0.1	0.4763
10	0.7761	0.6	0.6135
11	0.2432	0.2	0.2434
12	0.5459	0.5	0.5375
13	1	0.8	0.7133
14	0.6071	1	0.6444
15	0.3784	0.4	0.6319
16	0.5468	0.3	0.5841
17	0.2931	0.1	0.5413
18	0.6087	0.6	0.6077

Step 3: Δ_{ij} values have been calculated by using formula as mentioned in section 4.6.1. The values of Δ for different responses have been shown in Table 4.16.

Table 4.16: Δ value for various responses

S.No.	Δ for tensile strength	Δ for toughness	Δ for microhardness
1	0.4541	0.9	0.3388
2	1	1	0.7133
3	0.5692	0.8	0.3836
4	0.6586	0.9	0.3226
5	0.4767	0.6	0.257
6	0.4799	0.4	0.2585
7	0.6361	0.6	0.3461
8	0.8164	1	0.53
9	0.7661	0.9	0.237
10	0.2238	0.4	0.0998
11	0.7568	0.8	0.4699
12	0.4541	0.5	0.1758
13	0	0.2	0
14	0.3929	0	0.0689
15	0.6216	0.6	0.0814
16	0.4532	0.7	0.1292
17	0.7069	0.9	0.172
18	0.3913	0.4	0.1056

Step 4: After finding Δ, grey relation coefficient(Y) has been calculated. Its values for different responses are shown in Table 4.17

Table 4.17: Grey relation coefficient for various trials

S.No.	Y for tensile strength	Y for toughness	Y for microhardness
1	0.5241	0.3571	0.5128
2	0.3333	0.3333	0.3333
3	0.4676	0.3846	0.4818
4	0.4316	0.3571	0.5251
5	0.5120	0.4545	0.5812
6	0.5103	0.5556	0.5798
7	0.4401	0.4545	0.5075
8	0.3798	0.3333	0.4022
9	0.3950	0.3571	0.6008
10	0.6908	0.5556	0.7814
11	0.3978	0.3846	0.4315
12	0.5241	0.5	0.6698
13	1	0.7143	1
14	0.5600	1	0.8381
15	0.4458	0.4545	0.8142
16	0.5245	0.4167	0.7341
17	0.4143	0.3571	0.6746
18	0.5610	0.5556	0.7716

Step 5: Grey relation grade is calculated by taking the average of all grey relation coefficient. Table 4.18 shows the different input parameters value with corresponding grey grade.

Table 4.18: Grey relation grade at different parameters level

S.No.	Post weld aging	Current (A)	Voltage (V)	Gas flow rate (L/min)	Groove angle (degree)	Grey relation grade
1.	No	150	20	10	60	0.4647
2.	No	150	22	13	75	0.3333
3.	No	150	24	16	90	0.4447
4.	No	170	20	10	75	0.4379
5.	No	170	22	13	90	0.5159
6.	No	170	24	16	60	0.5485
7.	No	190	20	13	60	0.4674
8.	No	190	22	16	75	0.3718
9.	No	190	24	10	90	0.4509
10.	180° C,6 hour	150	20	16	90	0.6759
11.	180° C,6 hour	150	22	10	60	0.4046
12.	180° C,6 hour	150	24	13	75	0.5646
13.	180° C,6 hour	170	20	13	90	0.9048
14.	180° C,6 hour	170	22	16	60	0.7994
15.	180° C,6 hour	170	24	10	75	0.5715
16.	180° C,6 hour	190	20	16	75	0.5584
17.	180° C,6 hour	190	22	10	90	0.4820
18.	180° C,6 hour	190	24	13	60	0.6294

From Table 4.18, it is clear that the optimal result from different parameter level for different responses is trial condition 13 which has a highest value of 0.9048. With the help of this analysis, different parameters can be compared with the help of grey relational grade for multi objective responses . For optimal trial 13 the welding parameters are post weld aging , 170 A current, 20 V voltage, 13 L/min gas flow rate and groove angle is 90°. It has highest tensile strength value of 205.6 MPa and this sample contains second highest property in toughness. This result shows that post weld aging increase the tensile strength and toughness of joint. The reason is post weld aging increases the ductility and due to this tensile strength and toughness increase. The optimal result lies in range of 170A because higher current can cause burn out the plate and at lower current does not have lots of defect like porosity etc and fusion does not take place properly. For voltage, optimal results lie in the range of 20 V.

Higher voltage causes high heat input . Due to this its mechanical properties decrease . Gas flow rate and groove angle should lie in the range of 13L/min and 90° respectively. Grey relation analysis provide separate grade for each parameter combination. Thus we can compare each others.

4.7 Metallurgical study

For metallurgical study, weld plates were cleaned, polished and etched. Then sample was put under microscope. There are 3 zone in which study is done which are base metal zone, heat affected zone (HAZ) and fusion zone (FZ).

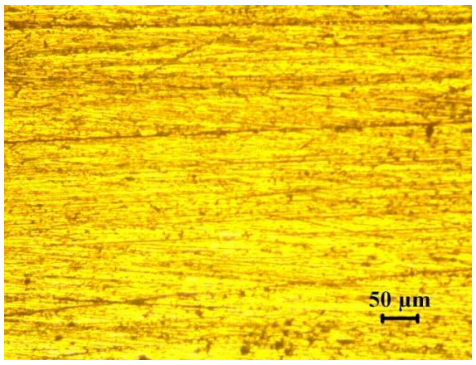

(a) Base metal

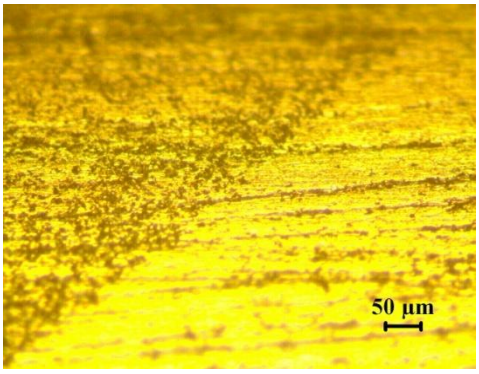

(b) FZ and HAZ for experiment trial 3

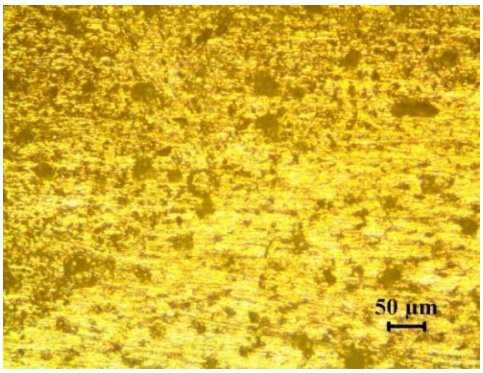

(c) FZ and HAZ for experiment trial 13

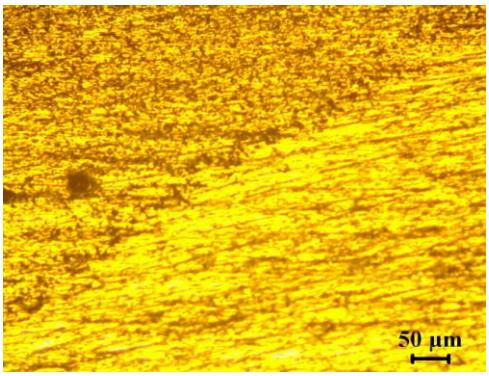

(d) FZ and HAZ for experiment trial 8

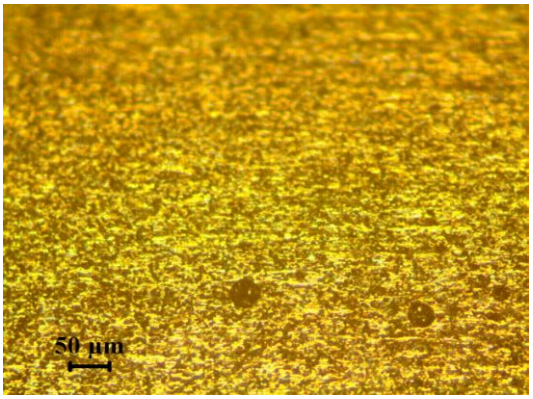

(e) FZ for experiment trial 6

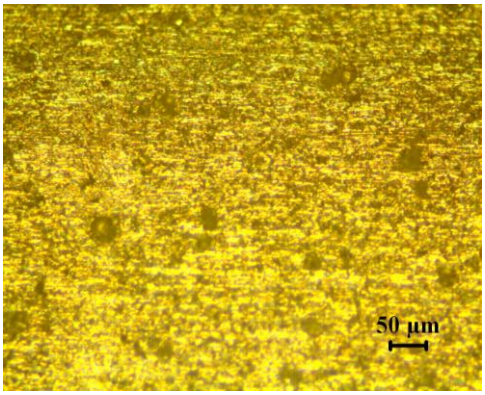

(f) FZ of experiment trial 13

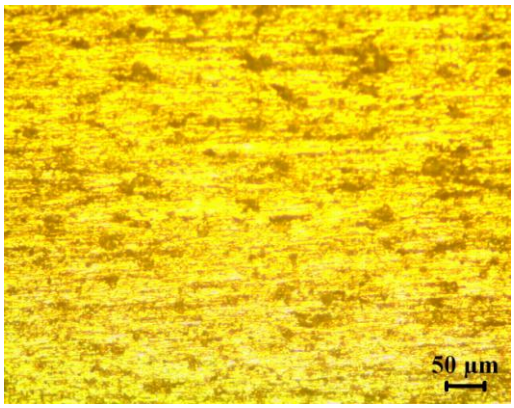

(g) HAZ for experiment trial 6

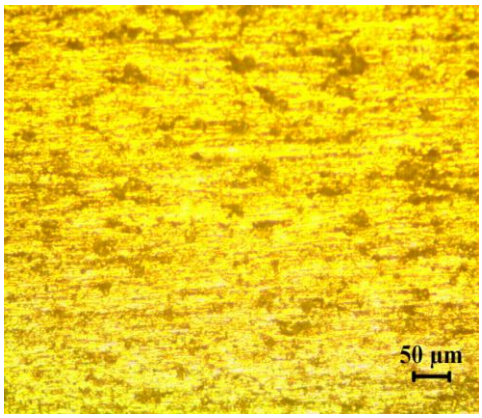

(h) HAZ for experiment trial 14

Fig 4.6: Optical microscope structure of weld joint for different experimental trial (Refer section 3.3 for experimental trial)

Fig 4.6 shows the microscope structure of Al 6063 weld joint at different. From the Fig 4.6 (a), it is clear that base metal consist of granular structure. Some Mg and Si alloys spots are found uniformly in this figure. In Fig 4.6 (b), Fig 4.6 (c), Fig 4.6 (d) both fusion zone and heat affected zone have been shown. These two zones can be easily understood in this figure because fusion exists in U shape area. It can be seen in the figure that in experiment trial 3 and 8, there are few precipitates. But for experimental trial 13, there are large precipitates of Mg_2Si. This is because post weld aging is applied for experimental trial 13. Fig 4.6 (e) and Fig 4.6 (f) shows the fusion zone for the different welding conditions. There is coarse granular structure in fusion zone. Fig 4.6 (g) and Fig 4.6 (f) shows the heat affected zone for different welding conditions. There is variation of precipitates according to welding parameters.

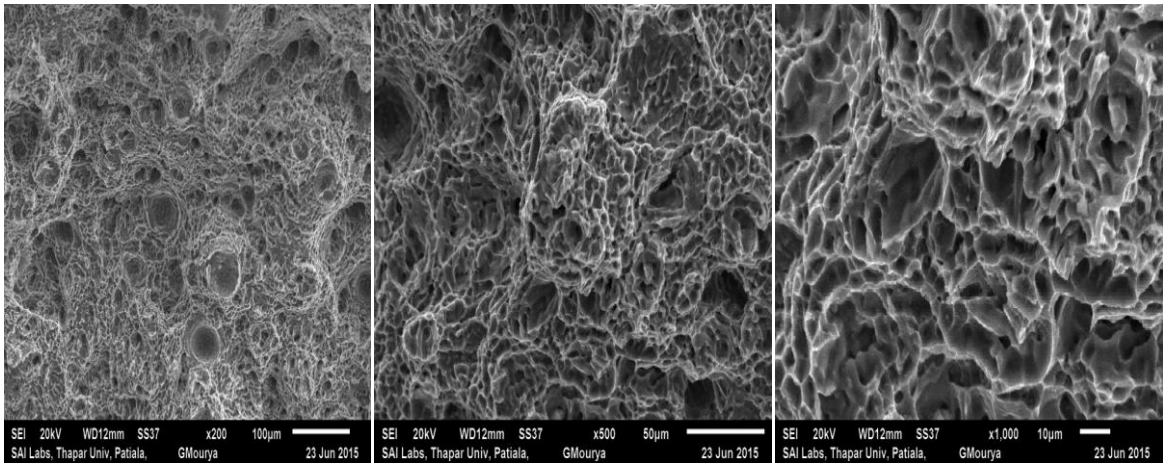

(a) (b) (c)

Fig 4.7: SEM pictures of fractured tensile specimen for experiment trial 13 at (a) 200x (b) 500x (c) 1000x (Post weld aging, 170 A, 20 V, 13 L/min, 90°)

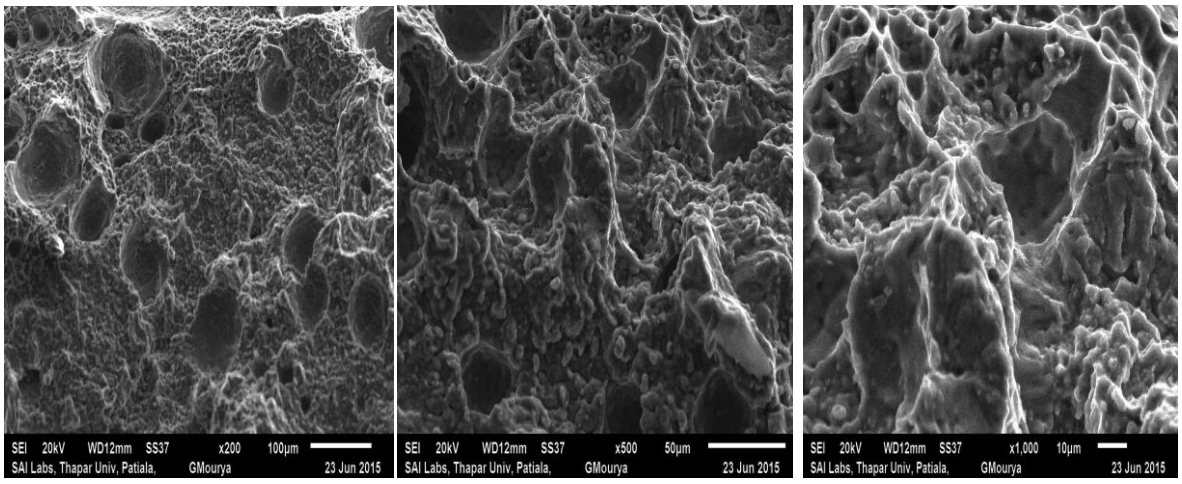

(a) (b) (c)

Fig 4.8: SEM pictures of fractured tensile specimen for experiment trial 2 at (a) 200x (b) 500x (c) 1000x (No aging, 150 A, 22 V, 13 L/min, 75°)

Fig 4.7 and 4.8 shows the SEM pictures of fractured tensile specimen at different magnification level. All tensile specimens have failed from the weld region. These figures show that fractured specimen have dimple structure which means that sample failed in ductile manner. The size of the dimples depends upon the welding condition used on that sample. There is a fine size of dimple in Fig 4.7 as comparison to Fig 4.8. This is the reason that experimental trial 13 has higher tensile strength. In these figure, there is inter granular fracture observed in both Fig 4.7 and Fig 4.8. This is because of combined effect of coarse

grained weld and precipitation of Mg_2Si present in the grain boundary. The value of tensile strength depends on the amount of Mg_2Si. The tensile strength of base metal is higher than the weld joint because in base metal the precipitates of Mg_2Si are uniformly distributed in the alloy. For neglecting solidification crack, the weld region has lesser amount of the precipitates so it has lesser tensile strength compare to base metal. The size of the dimple grain depends on heat input of the welding process. Higher heat input causes the less tensile strength. MIG welding generates higher heat input because it contains consumable electrode and filler metal is connected to positive polarity. That is why it generates high heat input. In SEM pictures, porosity is also shown. This also affects the tensile properties of weld joint. This should be less for higher strength.

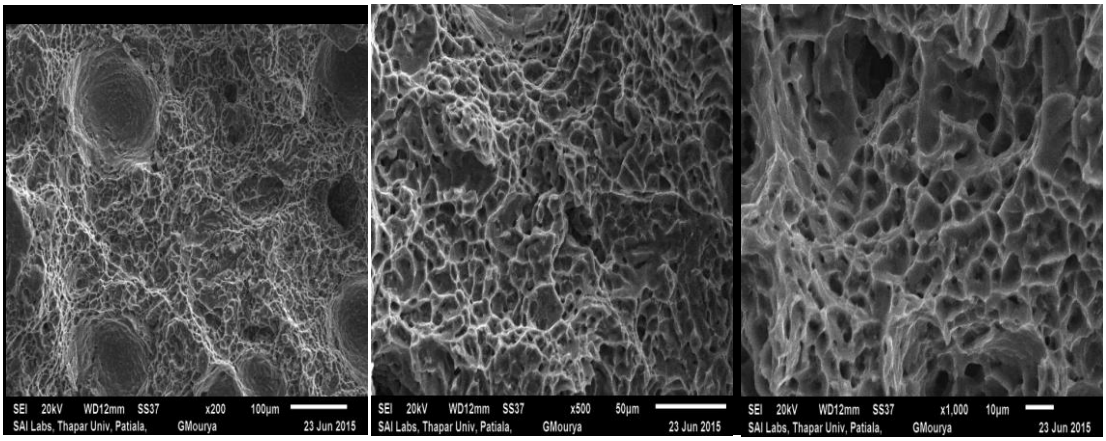

(a) (b) (c)

Fig 4.9: SEM pictures of fractured toughness specimen for experiment trial 14 at (a) 200x (b) 500x (c) 1000x (Post weld aging, 170 A, 22 V, 16 L/min, 60°)

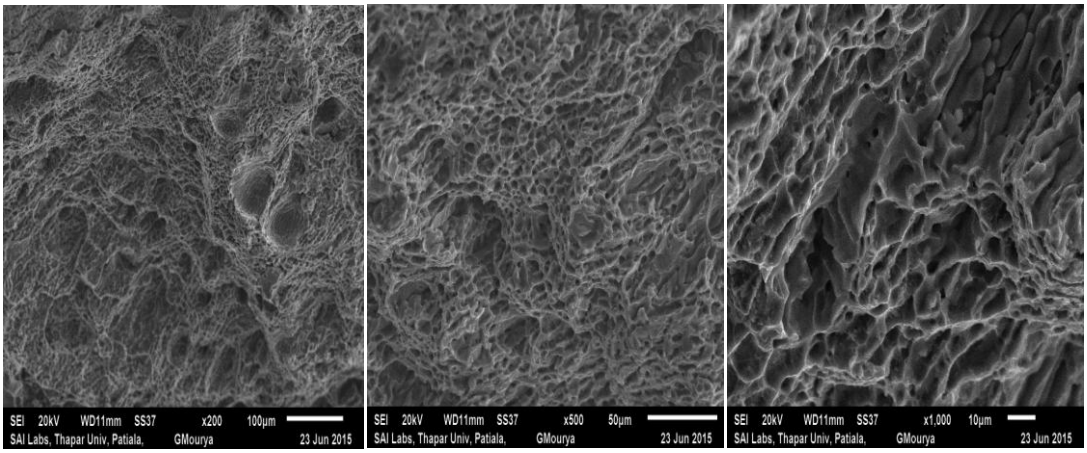

(a) (b) (c)

Fig 4.10: SEM pictures of fractured toughness specimen for experiment trial 2 at (a) 200x (b) 500x (c) 1000x (No aging, 150 A, 22 V, 13 L/min, 75°)

Fig 4.9 and Fig 4.10 shows the SEM pictures of fractured toughness specimen. There is intergranular structure for toughness fracture. There is a fine grain size of Fig 4.9 as compare to Fig 4.10. This is the reason why trial 14 has more toughness as compare to trial 2. For toughness specimen, failure takes place from the weld region. The toughness of the base metal is higher than the weld metal due to higher Mg_2Si precipitates distribution. The size of the grain depends upon the welding parameters. If welding parameter produces fine structure then that weld metal contains higher toughness.

CHAPTER-5

Conclusions and Scope for Future Work

5.1 Conclusions

Aluminium alloy Al-6063 plates were welded by MIG welding at different parameter levels. Taguchi method was used to optimize the welding parameter. Various tests were done on the weld joint to find out different mechanical properties of weld. The different outcomes of the test were utilized for the optimization study of the weld. For different outcomes, the best result for the experimental setup was found out by using Grey relation analysis. Some of the important features were observed in MIG welding which is discussed in this section.

- For tensile strength, voltage is the most significant factor for this experimental setup. Post weld aging increases the tensile strength. In this study, increasing the current tensile strength increases at a certain point but after that tensile strength reduces because excess penetration can melt the plate. On increasing the voltage tensile strength decreases because it produces higher heat input which reduces the strength. On increasing gas flow rate, tensile strength increases because it controls the heat input but after certain limit, it gives constant result. Groove angle also affects the strength of joint. The optimal solution of tensile strength lies in the range of 190.3 ± 14.39 MPa. For this result, plate with post aging and current in range of 170 A, voltage in range of 20 V, gas flow rate in range of 13 L/min and groove angle in range of 90̊ is required.
- For toughness, current is the most significant factor for this setup. Post weld aging increases the toughness of joint. In this study, increasing the current tensile strength increases at a certain point but after that tensile strength reduces because excess penetration can melt the plate. On increasing the voltage tensile strength decreases because it produces higher heat input which reduces the strength. On increasing gas flow rate, tensile strength increases because it controls the heat input but after certain limit, it gives constant result. Groove angle also affects the strength of joint. The optimal solution of tensile strength lies in the range of 12.215 ± 1.45 J. For this result,

plate with post aging and current in range of 170 A, voltage in range of 24 V, gas flow rate in range of 13 L/min and groove angle in range of 60̊ is required.

- For microhardness, post weld aging is the most significant factor. Besides this, current and voltage also plays a significant role. The optimal solution range for microhardness in fusion zone is 83.73 ± 4.96 VHN and in HAZ is 64.24 ± 3.97 VHN. The optimal parameters for this result lay in the range of 170 A, 20 V. For this post weld aging is also required.
- Base metal consists of fine equiaxed granular grain structure while weld zone consists of coarse grain structure. The base metal has higher tensile strength and toughness as compare to weld metal because it contains higher Mg_2Si precipitates while weld metal has less precipitates so their tensile strength and toughness are low. Due to aging some precipitates of Mg_2Si are formed in weld zone. This is why post weld aged sample has more tensile strength compare to weld metal but less strength compare to base metal. SEM fractographs of tensile specimen and toughness specimen consist of simple dimple structure. The size of grain depends on the welding parameters. Higher tensile strength sample has a fine grain size structure.
- From grey analysis it is found that for multi-response responses, the best optimal solution has been found in experiment trial 13 which is post weld aged, current -170 A, voltage- 20V, gas flow rate- 13L/min and groove angle- 90̊. This trial has highest tensile strength and second highest in toughness from all experiment trials.

5.2 Scope for future work

- By using the same factors and their levels, the simulation can be done for tensile strength or any other mechanical properties. The simulation result can be compared with experimental results.
- By using the MIG welding data, a mathematical model can be generated for heat distribution or inter metallic temperature distribution by using Finite element method.
- By using the same factors and data, other optimization techniques like RSM method, fuzzy logic can be applied and different results can be compared.
- By using the same parameters, cold spray method can be used for MIG welding and different results can be calculated for this.

References

- Aesh, M.A. (2007) Optimization of weld bead dimensions in GTAW of Al-Mg alloy. *Materials and Manufacturing Processes*, 16(5): 725-736
- Ahmad, R., Bakar, M.A. (2011) Effect of a post weld heat treatment on the mechanical and microstructure properties of AA6061 joints welded by the gas metal arc welding cold metal transfer method. *Materials and Design*, 32: 5120-5126
- Balasubramanian, V., Ravisankar, V., Madhushudhan, G. (2007) Effect of pulsed current welding on fatigue behavior of high strength aluminum alloy joints. *Materials and Design*, 29: 492-500
- Cheema, G.S., Singh, N., Singh, G., Singh Kang, A. (2014) Influence of post weld heat treatment on mechanical and metallurgical properties of TIG welded aluminum alloy joints. *Internation Journal of Chemical, Nuclear, Materials and Metallurgical Engineering*, 8(12): 1241-1244
- Dongxia, Y., Xiaoyan, L., Zuoren, N., Dingyong, H., Hui, H., Guanzhen, Z. (2012) Microstructure characteristics of TIG welded Al-Mg alloy with small amount Er addition . *Rare Metal Materials and Engineering*, 41(10): 1713-1716
- Dutta, P., Pratihar, D.K. (2006) Modeling of TIG welding process using conventional regression analysis and neural network- based approaches. *Journal of Materials Process Technology*, 184: 56-68
- Firouzdor, V., Kou, S. (2010) Formation of liquid and inter metallic in Al-to-Mg friction stir welding. *Metallurgical and material transfer*, 41(A): 2914-2935
- Ghosh, P.K., Dorn, L., Hubner, M., Goyal, V.K. (2007) Arc characteristics and behavior of metal transfer in pulsed current GMA welding of aluminum alloy. *Journal of Material Process Technology*, 194: 163-175
- Guo, H., Hu, J., Tsai, H. (2009) Formation of weld crater in GMAW of aluminum alloys. *International Journal of Heat and Mass transfer*, 52: 5533-5546

- Jong kim, S., Kweon kim, S., Cheul park, J., (2010) The corrosion and mechanical properties of Al alloy 5083 –H116 in metal inert gas welding based on slow strain rate test. *Surface & coating Technology*, 205: S73-S78
- Kumar, A., Sundarrajan, S. (2008) Optimization of pulsed TIG welding process parameters on mechanical properties of AA5456 Aluminum alloy weldments. *Materials and Design*, 30: 1288-1297
- Lakshminarayan, A.K., Balasubramanian, V., Elangovan, K. (2007) Effect of welding process on tensile properties of AA6061 aluminum alloy joints. *International Journals of Advanced manufacturing Technology*, 40: 286-296
- Li, D., Lu, S., Dong, W., Li, D., Li, Y. (2011) Study of the law between the weld pool shape variations with the welding parameters under two TIG processes. *Journals of Materials Processing Technology*, 212: 128-136
- Maggiolino, S., Schmid, C. (2007) Corrosion resistance in FSW and MIG welding techniques of AA6xxx. *Journal of Materials process Technology*, 197: 237-240
- Manti, R., Dwivedi, D.K. (2007) Microstructure of Al–Mg–Si Weld Joints Produced by Pulse TIG Welding, *Materials and Manufacturing Process*, 22(1): 57-61
- Mathivanan, A., Devakumaran, K., Kumar, A.S. (2014) Comparative study on mechanical and metallurgical properties of AA6061 aluminum alloy sheet weld by pulsed current and dual pulse gas metal arc welding process. *Materials and Manufacturing Process*, 29: 941-947
- Mutombo, K., Dutoit, M.(2011) Corrosion fatigue behavior of aluminium alloy 6061-T651 welded using fully automatic gas metal arc welding and ER5183 filler alloy. *International Journal of Fatigue*, 33: 1539-1547
- Qin, G., Su, Y., Meng, X., Fu, B. (2015) Numerical simulation on MIG arc brazing – fusion welding of aluminum alloy to galvanized steel plate. *International Journals of Advanced Manufacturing Technology*, 78: 1917-1925

- Rui, W., Zhenxin, L., Jianxun, Z. (2008) Experimental Investigation on Out-of-Plane Distortion of Aluminum Alloy 5A12 in TIG Welding. *Rare Metal Materials and Engineering*, 37(7): 1264-1268
- Salazar, J.M., Urena, A., Villauriz, E., Manzanedo, S., Barrena, I. (2010) TIG and MIG welding of 6061 and 7020 aluminium alloys micro structural studies and mechanical properties. *Welding International,* 13(4): 293-295
- Senthil, T.K., Balasubramanian, V., Sanavullah, M.Y. (2006) Effect of pulsed current TIG welding parameters on pitting corrosion behavior of AA6061 Aluminum alloy. *Journal of Material Science Technology*, 23(2): 223-229.
- Shiang, S.J., Fong, T.y., Bin, Y.J. (2011) Principle component analysis for multiple quality characteristics optimization of metal inert gas welding aluminum foam plate. *Materials and Designs*, 32: 1253-1261
- Sugamata, M., Kaneko, J., (2010) Mechanical properties of TIG welded joints on heavy AZ31 magnesium alloy plates, *Welding International,* 21(2): 103-109
- Temmar, M., Hadji, M., Sahrouli, T. (2011) Effect of post weld-aging treatment on mechanical properties of Tungsten inert gas welded low thickness 7075 Aluminum alloy joints. *Materials and design* , 32: 3532-3536
- Traidia, A., Roger, F. (2011) Numerical and experimental study of arc and weld pool behavior for pulsed current GTA welding. *International Journal of Heat and Mass Transfer,* 54: 2163-2179
- Vargas, J.A., Torres, J.E., Pacheco, J.A., Hernandez, R.J. (2013) Analysis of heat input effect on the mechanical properties of Al-6061-T6 alloy weld joints. *Materials and design*, 52: 556-564
- Wei, S., Li, Y., Wang, J., Liu, K. (2014) Influence of welding heat input on microstructure of Ti/Al joint during pulsed gas metal arc welding. *Materials and Manufacturing Processes*, 29: 954-960

- Yan, S., Nie, Y., Zhu, Z., Chen, H., Gou, G., Yu, J., Wang, G. (2014) Characteristics of microstructure and fatigue resistance of hybrid fiber laser-MIG welded Al-Mg alloy joints. *Applied Surface Science*, 298: 12-18
- Zhao, J., Jiang, F., Jian, H., Wen, K., Jiang, L., Chen, X. (2010) Comparative investigation of tungsten inert gas and friction stir welding characteristics of Al-Mg-Sc alloy plates, *Materials and Design*, 31: 306-311

Web References

Web reference 1: http://resource.npl.co.uk/mtdata/phdiagrams/almg.htm

Appendix

Graphs between stress and strain

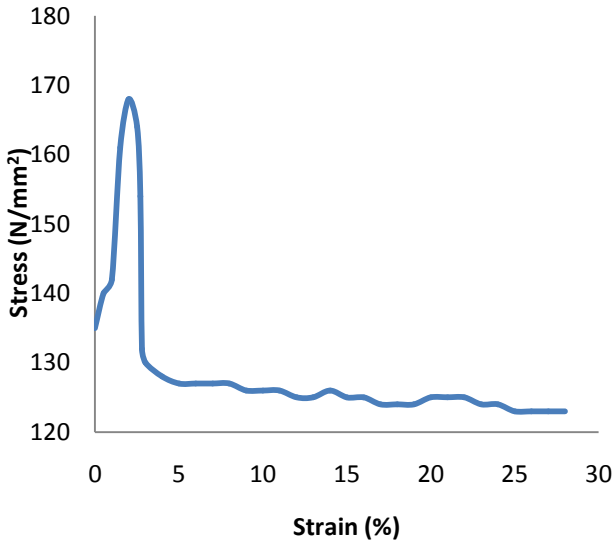

Stress – Strain curve for E-1 experiment

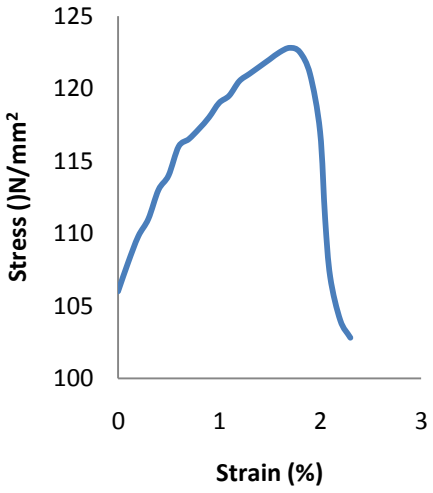

Stress – Strain curve for E-2 experiment

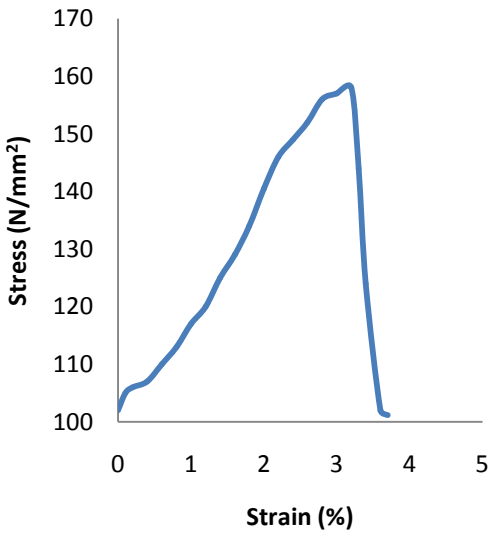

Stress – Strain curve for E-3 experiment

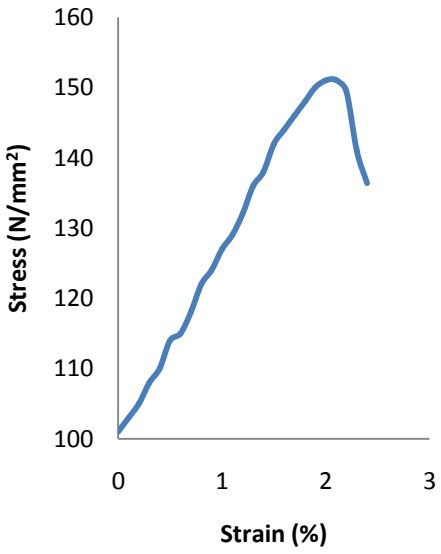

Stress – Strain curve for E-4 experiment

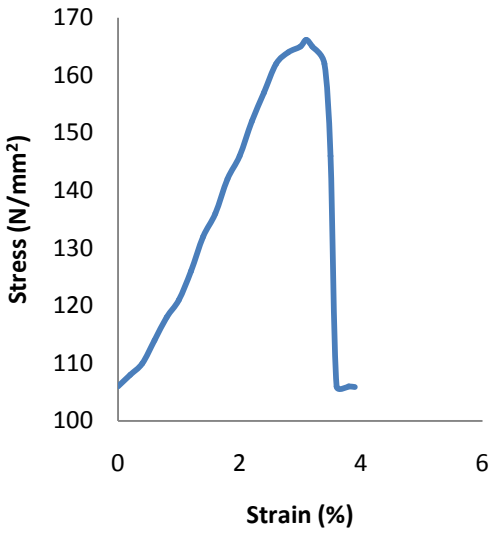

Stress – Strain curve for E-5 experiment

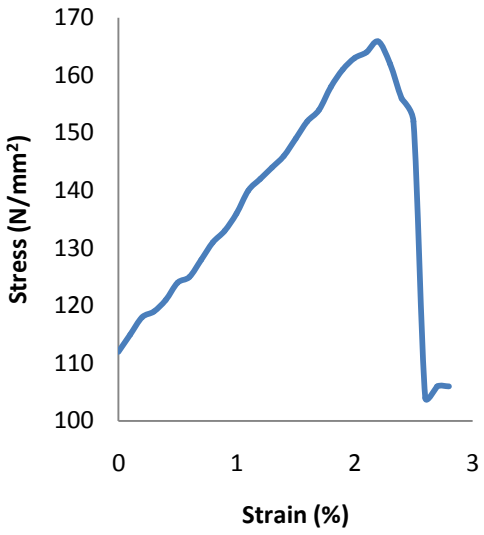

Stress – Strain curve for E-6 experiment

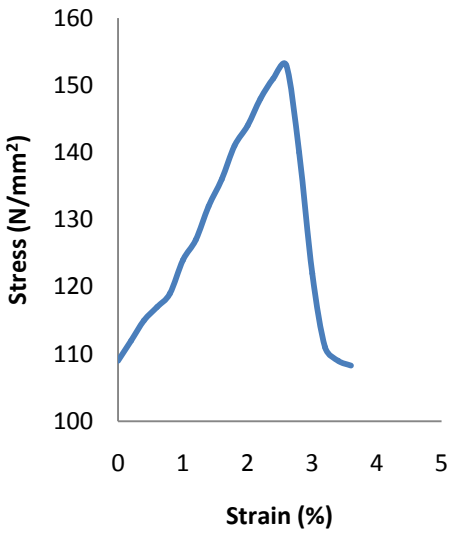

Stress – Strain curve for E-7 experiment

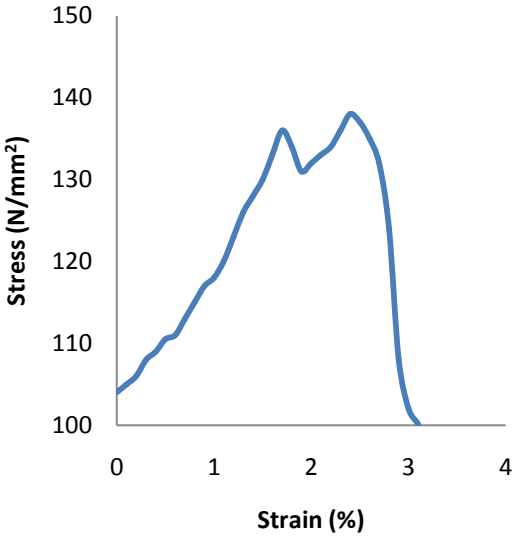

Stress – Strain curve for E-8 experiment

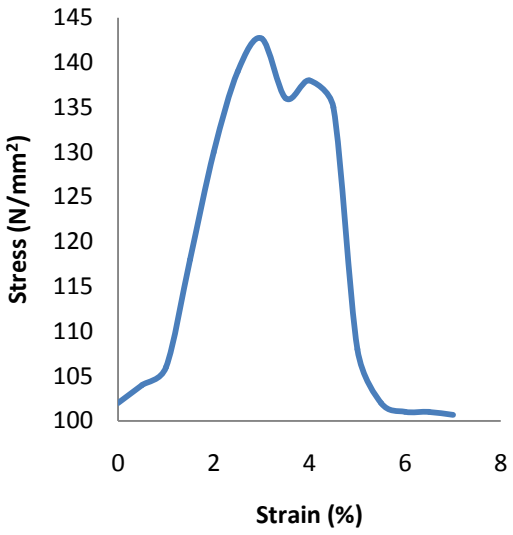

Stress – Strain curve for E-9 experiment

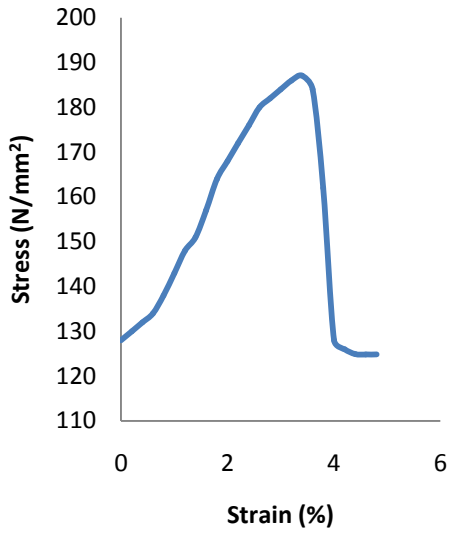

Stress – Strain curve for E-10 experiment

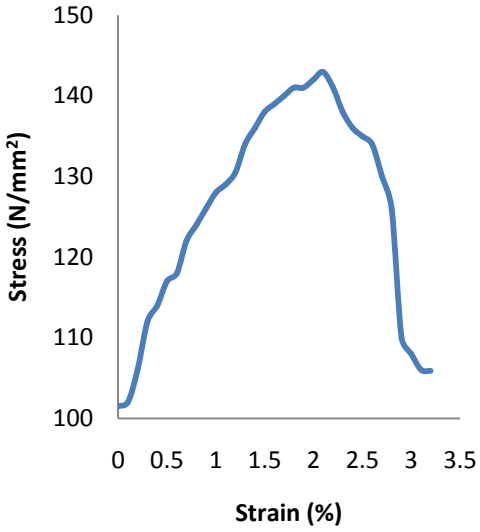

Stress – Strain curve for E-11 experiment

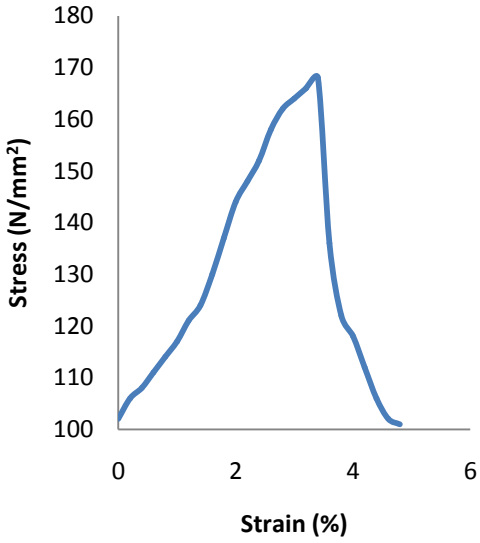

Stress – Strain curve for E-12 experiment

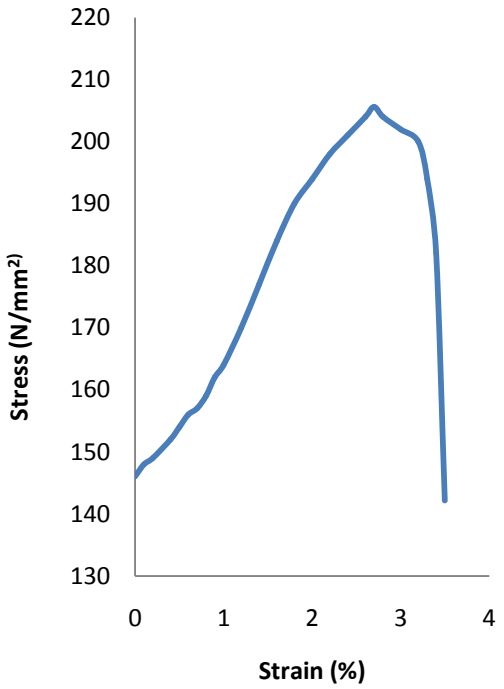

Stress – Strain curve for E-13 experiment

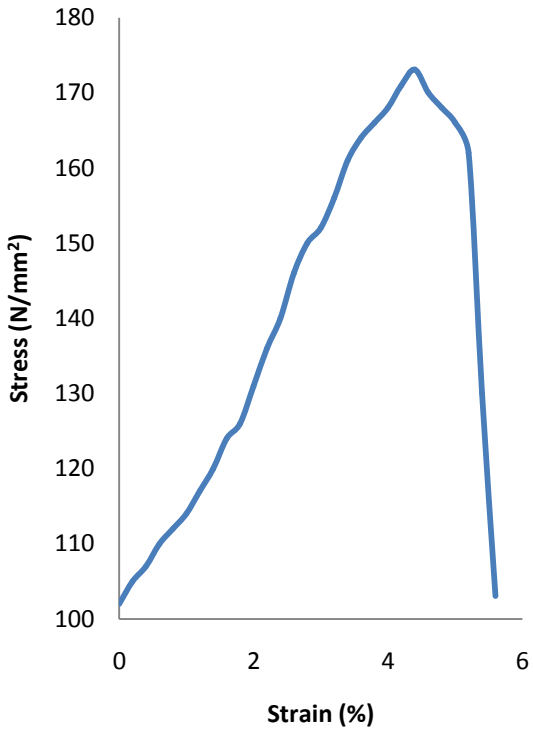

Stress – Strain curve for E-14 experiment

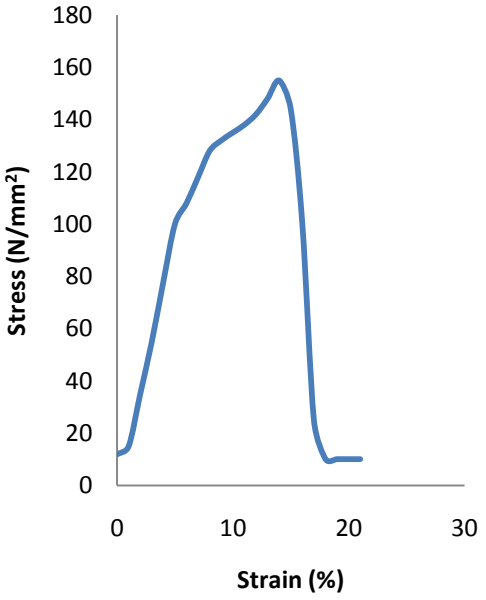

Stress – Strain curve for E-15 experiment

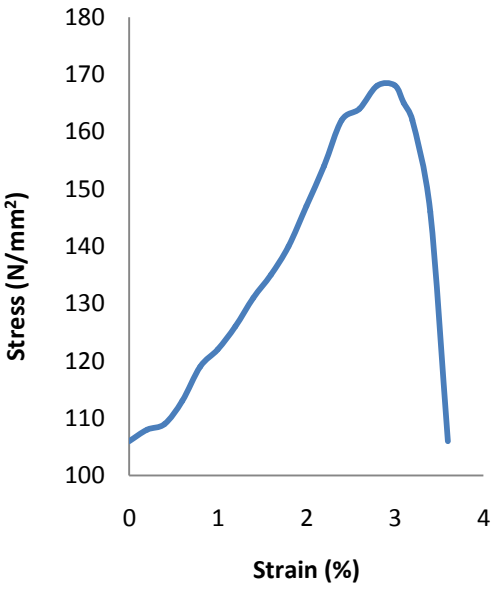

Stress – Strain curve for E-16 experiment

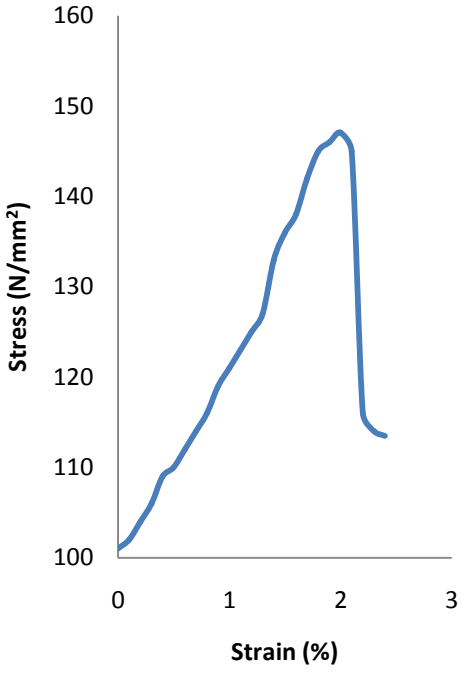

Stress – Strain curve for E-17 experiment

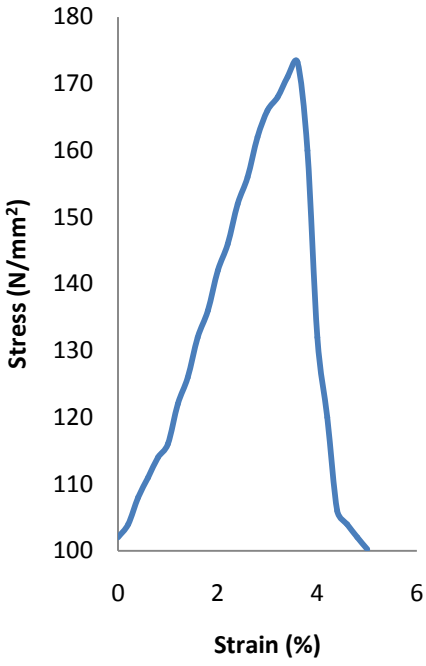

Stress – Strain curve for E-18 experiment